



Institución Universitaria

**Automatic swallowing analysis based
on accelerometry and surface
electromyography**

Juan Pablo Restrepo Uribe

Instituto Tecnológico Metropolitano - ITM
Facultad de Ingenierías. Departamento de Electrónica y Telecomunicaciones
Medellín, Colombia
2021

Análisis automático de la deglución basado en acelerometría y electromiografía de superficie

Juan Pablo Restrepo Uribe

Trabajo de grado presentado como requisito parcial para optar al título de:
Magíster en Automatización y Control Industrial

Directores:

MSc. Sebastián Roldán Vasco
PhD. Andrés Felipe Orozco Duque

Línea de Investigación:

Biomateriales y Electromedicina

Grupo de Investigación:

Grupo de Investigación en Materiales Avanzados y Energía MATyER

Instituto Tecnológico Metropolitano
Facultad de Ingenierías, Departamento de Electrónica y Telecomunicaciones
Medellín, Colombia
2021

“... Es muy largo el camino
Para mirar atras
Que más da...”

Joan Manuel Serrat

“One never notices what has been done; one
can only see what remains to be done”

Marie Skłodowska Curie

Acknowledgements

I want to start by thanking Sebastián Roldán Vasco and Andrés Felipe Orozco Duque, who accompanied me and guided me in the best way. Also, a special thanks to my family who always supported me in every step taken. Appreciate that they understood my absence and silence in important moments for everyone. I have no words to express gratitude to the one who accompanied me almost from the beginning, who knew how to give me words of encouragement and gave me his company. Finally, I want to thank the ITM and the UPB for supporting this process with technical resources that allowed the completion of this work. Without this support, none of this would have been possible. I thank the Ministry of Sciences for the financing of the project 121077758144 of 2017 in which this research is framed.

A special thanks to the one who is no longer with me, but made this possible, I also thank him for showing me that education changes lives.

Abstract

Swallowing is a complex act that involves different anatomical structures. Neurological or physical alterations can change this process and produce a symptom known as dysphagia. It is estimated that it affects around 16 % of the population worldwide. The diagnosis of this symptom focuses on invasive techniques such as videofluoroscopy and fiberoptic endoscopy. This motivates the development of non-invasive, low-cost, and safe techniques. Recently, accelerometry (ACC) and surface electromyography (sEMG) signals have been investigated separately for dysphagia screening purposes, with promising results. However, they analyze swallowing as a one-dimensional process, ignoring its complexity. Thereby, a methodology was developed for the analysis of ACC and sEMG signals jointly and synchronously. For this, healthy and dysphagia subjects were given water and yogurt. These signals were filtered and characterized by the sliding window method. Filtering methods were implemented to select the features that retrieved maximum separability between classes. For all swallowing tasks evaluated by applying classifiers, areas under the ROC curve (AUC) and sensitivities higher than 0.85 were obtained. The best-case corresponded to 20 mL of water, with an AUC of 0.91. The implemented methodology made it possible to determine that multi-sensor fusion improves the results regarding the use of signals independently. The proposed methodology is promising for dysphagia screening in an objective and non-invasive way.

Keywords: accelerometry, biomedical signal processing, classification algorithms, dysphagia, feature extraction, feature selection, electromyography, swallowing

Resumen

La deglución es un acto complejo que involucra diferentes estructuras anatómicas. Las alteraciones neurológicas o físicas pueden alterar este proceso y desarrollar un síntoma conocido como disfagia. Se estima que afecta a alrededor del 16% de la población mundial. El diagnóstico de este síntoma se centra en técnicas invasivas como la videofluoroscopia y la endoscopia de fibra. Esto motiva el desarrollo de técnicas seguras, no invasivas y de bajo costo. Recientemente, las señales de acelerometría (ACC) y electromiografía de superficie (sEMG) se han investigado por separado con fines de tamización de disfagia, con resultados prometedores, sin embargo, analizan la deglución como un proceso unidimensional, ignorando que es complejo e involucra diferentes estructuras. Debido a esto se desarrolló una metodología para el análisis de ambas señales de forma conjunta y sincrónica. Para ello, se adquirieron señales ACC y sEMG mientras sujetos sanos y con disfagia deglutían agua y yogur. Estas señales se filtraron y caracterizaron mediante el método de ventana deslizante. Se implementaron métodos de filtro para seleccionar las características que recuperaron la máxima separabilidad entre las clases. Para todas las tareas deglutorias evaluadas mediante la aplicación de clasificadores, se obtuvieron áreas bajo la curva ROC (AUC) y sensibilidades superiores a 0.85. El mejor de los casos correspondió a 20 ml de agua, con un AUC de 0.91. La metodología implementada permitió determinar que la fusión multisensor mejora los resultados frente al uso de señales de forma independiente, resultando así en una metodología prometedora para la tamización de la disfagia de forma objetiva y no invasiva.

Palabras clave: acelerometría, algoritmos de clasificación, deglución, disfagia, electromiografía, extracción de características, selección de características, procesamiento de señales biomédicas

Content

Acknowledgements	v
Abstract	vi
Figure list	ix
Table list	x
1. Introduction	2
1.1. Justification	2
1.2. Swallowing	3
1.3. Dysphagia	4
1.3.1. Diagnosis of dysphagia	4
1.4. State of the art	6
1.4.1. Electromyography	6
1.4.2. Accelerometry based cervical auscultation (ACC)	8
1.4.3. Multi-sensor fusion	9
1.5. Problem statement	10
1.6. Objectives	10
1.6.1. General objectives	10
1.6.2. Specific objectives	10
2. Materials and methods	12
2.1. Subjects	12
2.1.1. Healthy subjects	12
2.1.2. Dysphagic subjects	12
2.2. Data acquisition	14
2.2.1. Surface electromyography	14
2.2.2. Accelerometry	15
2.2.3. Synchronization	15
2.2.4. Signal recording	16
2.3. Pre-processing	17
2.3.1. ACC pre-processing	18
2.3.2. EMG pre-processing	19

2.4.	Feature extraction	19
2.4.1.	Time domain	19
2.4.2.	Frequency domain	21
2.4.3.	Time-frequency domain	21
2.4.4.	Information-theoretic features	22
2.4.5.	Statistical moments and signal segmentation for the feature extraction	23
2.5.	Feature selection	25
2.6.	Classification and optimization	28
2.6.1.	Classification	28
2.6.2.	Optimization	33
2.6.3.	Model selection	34
3.	Results	37
3.1.	Acquisition of ACC signal	37
3.1.1.	Custom software MODAC	37
3.2.	Pre-processing	39
3.2.1.	Wavelet denoising	39
3.3.	Feature extraction and feature selection	41
3.4.	Classification	45
3.5.	Model selection	55
4.	Conclusions and contributions	60
4.1.	Conclusions	60
4.2.	Limitations and future works	61
A.	Appendix: MODAC block diagram	62
	Bibliography	63

Figure list

1-1. Major muscles of swallowing	6
2-1. General methodology	12
2-2. Synchronization diagram	16
2-3. Acquisition protocol	16
2-4. Location of sEMG electrodes and accelerometer	17
2-5. Typical ACC signal	19
2-6. Sliding window in ACC signals.	23
2-7. Manual segmentation of signals	24
2-8. Feature extraction scheme	25
2-9. Principal components analysis	25
2-10. Mutual information	27
2-11. ROC curve	28
2-12. Support vectors and the separation hyperplane	30
2-13. Neural network	30
2-14. Neuron structure	31
2-15. XGBoost graphical representation	32
2-16. KNN graphical representation	33
2-17. Structure of matrix confusion	34
2-18. Methodological flowchart.	36
3-1. MODAC main window	37
3-2. Synchronization module	38
3-3. MODAC front panel	39
3-4. Spectrograms of swallowing and noise signals	41
3-5. Channels selected by task	43
3-6. Number of features selected per swallowing tasks	44
3-7. AUC highest	53
3-8. ROC curve for test subjects	58
A-1. MODAC block diagram	62

Table list

1-1. Common etiologies of oropharyngeal dysphagia	4
2-1. Inclusion and exclusion criteria	13
2-2. Demographic data. The average age and deviation of each group are reported. Where: M is male, and F female	14
2-3. Main characteristics of Noraxon Ultium EMG	14
2-4. NI-USB 6215 DAQ Multifunction device highlights	15
2-5. Number of analyzed boluses per population group	17
2-6. Time domain features	20
2-7. Frequency domain features	21
2-8. Time-frequency features	21
2-9. Information-theoretic features	22
3-1. Best wavelet denoising parameter	40
3-2. Number of features per swallowing task and feature domain	44
3-3. Classification results Y5	46
3-4. Classification results Y10	47
3-5. Classification results Y20	48
3-6. Classification results S	49
3-7. Classification results A5	50
3-8. Classification results A10	51
3-9. Classification results A20	52
3-10.MLP hyperparameters	56
3-11.XGBoost hyperparameters	56
3-12.SVM hyperparameters	56
3-13.Classification of test subjects	57
3-14.Performance measures with the test database	58

1. Introduction

1.1. Justification

Swallowing is a complex activity that is involved in the digestive process. Its complexity is due to the fact that it requires coordination of different systems, and it involves physiological activities, mainly of the neurological system with the intervention of five cranial nerves, and the muscular system with approximately thirty muscle pairs in the head, neck and chest [1, 2, 3]. Disturbances or lack of coordination of these two systems cause a symptom known as dysphagia. Swallowing has three phases: oral, pharyngeal, and esophageal [4, 5, 6]. Oropharyngeal dysphagia is a symptom of different diseases such as Alzheimer's, Parkinson's, myasthenia gravis, stroke, among others [2, 7, 8]. Patients diagnosed with dysphagia are commonly affected by malnutrition, dehydration, and laryngeal aspiration [9, 2, 7].

There is international concern around preventable deaths and respiratory illnesses from dysphagia [10]. Some research papers estimate the prevalence of dysphagia in approximately 16 to 22 % of the general population [7]. The prevalence in primary care is greater in women than in men [11, 12], which makes it important to consider that factors such as race, sex, and culture (associated with diet and eating habits) can become a risk factor for dysphagia. Similarly, the pathologies associated with dysphagia have variable epidemiological data. China evaluated dysphagia in Parkinson's disease and estimated that approximately 87.1 % of the population studied has dysphagia [13]. For intellectual disabilities, a tentative indication of the prevalence of dysphagia was found to be close to 8.15 % [14]. In the case of stroke, it is estimated that about 47 % of patients develop dysphagia for a short period, however, in a few of these patients dysphagia persists [15]. Appropriate and early diagnosis or treatment increases the life expectancy of patients [16].

There are three types of tests that assess swallowing of patients: screening (e.g. Eating Assessment Tool-10 (EAT-10)), clinical bedside swallow examinations (e.g. 3 oz water test), and instrumental tests such as the fiberoptic endoscopic evaluation of swallowing (FEES), which in some cases can cause discomfort, retching, vomiting, perforation of the mucosa, adverse reactions to topical anesthetics, among others [17]. Or the videofluoroscopic swallow study (VFSS), considered the instrumental gold standard, that is invasive, requires X-ray doses [18], which limits the follow-up evaluation. Furthermore, the cost per session is estimated between 200 and 500 USD [19].

1.2. Swallowing

Is the process where food and drink are ingested and transported to the stomach while preventing aspiration into the airway [20, 5, 21]. Swallowing involves different anatomical structures and physiologic processes at muscular, mechanical, and neurological levels. It also involves respiratory, digestive, and neurological systems. Coordination of the swallowing process is paramount to protect the respiratory system, including the coordination of the brain stem, cortical central pathways, and nervous systems [5]. The swallowing takes place in the upper gastrointestinal tract and involves three phases, where the bolus is formed and carried to the stomach. These are described below.

- **Oral:** This is the first phase of swallowing. Consists of different muscular activations that help break the foods, mix them with saliva, bolus formation, and transporting them from the mouth to the pharynx. This phase involves oral, supra, and infrahyoid muscles [22, 23, 24, 25]. In the oral phase, the following events occur:
 - Mouth opening
 - Entry of food into the mouth
 - Chewing
 - Bolus formation
 - Stimulation of the tonsillar pillars
- **Pharyngeal:** Involves a process with voluntary and involuntary control. The pharyngeal phase initiates when the bolus reaches the pharynx and started pharyngeal peristalsis, relaxation of the upper esophageal sphincter, and closure of the glottis, protecting the airway from aspiration [23, 25].
- **Esophageal:** It is considered the last phase of swallowing. In this phase, the bolus is carried from the esophagus to the lower esophageal sphincter [23, 25]. It is characterized by the following events:
 - Esophageal peristalsis
 - Relaxation of the lower esophageal sphincter
 - The pharynx and larynx return to their normal position
 - The air enters the lower airways again.

1.3. Dysphagia

Normal swallowing can be affected by alterations in anatomical structures, aging, radiation therapy, or neurological diseases. These alterations can produce a symptom known as dysphagia, which is characterized to affect the oral-transit time, the motility in all swallowing phases, and to produce piecemeal deglutition in solids and liquids [26, 27, 28, 29, 30]. Dysphagia is present in any phase of swallowing (oral, pharyngeal, or esophageal). Commonly, the dysphagia in oral and pharyngeal phases are analyzed jointly as oropharyngeal dysphagia. Oropharyngeal dysphagia is commonly associated with different diseases of central neurogenic or neuromuscular etiology (see Table 1-1).

Table 1-1. Common etiologies of oropharyngeal dysphagia

Central neurogenic etiology	Neuromuscular etiology
Ischemic stroke	Inflammatory myopathies
Hemorrhagic stroke	Muscular dystrophy
Multiple sclerosis	Myasthenia gravis
Motor neuron disease	Neuropathy
Dementia	
Traumatic brain injury	
Neuromyelitis	
Cerebral palsy	

The identification of risk factors in patients and the early diagnosis of dysphagia is important because it allows the design of treatments that are tailored to the needs of patients, and reduce the complications that can occur such as malnutrition, dehydration, aspiration pneumonia, and eventually, the death [31]. Although there is no cure for dysphagia, patients treated by multidisciplinary teams have shown improvements in their quality of life [32].

1.3.1. Diagnosis of dysphagia

Involves different techniques and methodologies. The instrumental tests are based on costly methods with associated risks; the screening and clinical bedside swallow examination are dependent on the experience of the treating personnel. The methods include:

- Screening
 - Physical exploration: Evaluates different structures and functions of swallowing. It seeks to determine alterations in the dentition, oral mucosa, presence of masses, or modifications in salivation. Likewise, aspects such as changes in the face-caudal and evaluation of motor and sensory functions are analyzed [33].

-
- Eating Assessment Tool-10: Recently the EAT-10 has gained popularity, due to its simplicity, and because it is applicable in a variety of swallowing disorders. The use of EAT-10 has shown that it is a useful tool to establish the severity of the patients [34, 33].
- Clinical bedside swallow examination
 - Evan's methylene blue test: Is used in patients of tracheostomy, it uses methylene blue in the tongue and evaluates the secretions in the next hours. It allows identifying aspirations, by evaluating if saliva passes from the pharynx to the trachea [33].
 - Blood glucose in bronchial secretions: Evaluates aspirations in tracheostomized patients, looking for the presence of glucose in secretions [33].
 - Instrumental diagnosis
 - Fiberoptic endoscopic evaluation of swallowing (FEES): Evaluates the swallowing, by introducing an endoscope while the patient eats food. The main limitations of the method are the space where the test is performed, which must be aseptic; the patient must be anesthetized, and it is not always possible to complete the test due to patient discomfort [35, 7]. It also has limitations such as that in some cases the patient may present cough, discomfort, gagging and/or vomiting, adverse reactions to the topical anesthetic or the methylene blue, anterior or posterior epistaxis, laceration of mucosal, or vasovagal episodes, also, only study the pharyngeal phase [17].
 - Video Fluoroscopic Swallowing Study (VFSS): It is considered the instrumental gold standard for the diagnosis of dysphagia. The test consists of bringing patients to doses of X-rays while they consume food with barium as a contrast medium. The test evaluates the different phases of swallowing, and it allows to identify the existence of reflux, bronchoaspiration, slowness, among other important pathological aspects [18].
 - Manometry: The manometry consists of inserting a pressure-sensitive probe through the mouth or nose. The test is mainly used to diagnose esophageal dysphagia, in some cases, it is used to diagnose oropharyngeal dysphagia, especially when upper esophageal sphincter dysfunction is suspected. The method is invasive [33].
 - Radioisotope transit: The technique is mainly used for the diagnosis of esophageal dysphagia, in the oropharyngeal dysphagia is not considered a sensitive and specific test [33].

1.4. State of the art

1.4.1. Electromyography

It is a widely used technique for the study of polarization and depolarization of muscle cells [36]. Needle or surface electrodes can be used, the latter being a non-invasive alternative known as surface electromyography (sEMG), where silver chloride electrodes (Ag/AgCl) are placed on the muscle regions of interest [37]. sEMG has been proposed as a technique that can provide useful information about swallowing [38]. It is a reproducible and inexpensive test [33]. The most commonly evaluated muscles in swallowing are the temporal muscle, which is mainly responsible for chewing; the orbicularis oris muscle, which has two portions, marginal portion, and labial portion, and is responsible for closing and opening the lips; in addition, the suprahyoid muscles, i.e. digastric anterior and posterior belly, geniohyoid, stylohyoid and mylohyoid muscles, which contribute mainly to the functions of the tongue and the laryngeal ascent; and finally the infrahyoid muscles, i.e. the sternohyoid, sternothyroid, thyrohyoid and omohyoid, which are attached to the hyoid bone and are responsible for its ascent and descent, as well the larynx; [39, 40, 38, 41, 42, 43]. Figure 1-1 shows the supra and infrahyoid muscles.

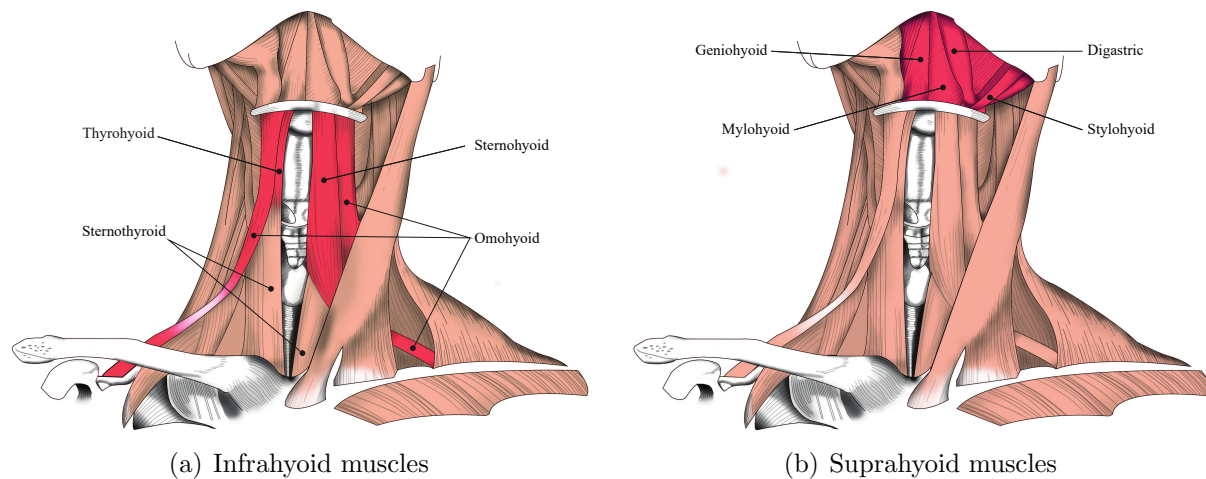


Figure 1-1. Location of the suprahyoid and infrahyoid muscles, and the cricoid cartilage. Modified from [44]

Most of the researches carried out in the field of sEMG to evaluate swallowing has focused on the analysis of the amplitude and timing of muscular activation with visual and statistical techniques [45, 46, 47]. Some researches have focused on the analysis of the mastication process [45] and the identification of normal muscular behavior [46]. Furthermore, the evaluation of the submental muscles in patients with Huntington's disease who present swallowing difficulties is highlighted [47]. Many researchers have focused on identifying the *onset* (start)

and *offset* (end) of the swallow-related signal and muscle activation times using statistics, in addition to the evaluation of the correlation between the muscle pairs analyzed [48, 49, 42]. However, the automatic evaluation of dysphagia is scarce.

The frequency content of muscle activity has been widely reported, and it has been established that the highest energy spectral density is located between 10 and 500 Hz [50, 51]. However, it has been found that swallowing muscles seem to have a limited bandwidth. According to Restrepo-Agudelo et al. (2017), the optimal filtering range for the sEMG signal of infrahyoid muscles is between 130 and 180 Hz [52]. However, in other studies filters with cut-off frequencies between 90 and 250 Hz have been implemented for these muscle groups [38]. Similarly, some signal filtering stages consisted of the implementation of Wavelet filters [38, 52].

Other studies have reported methodologies to detect muscle activation in swallowing through automation techniques. Restrepo-Agudelo et al. (2017) evaluated the automatic burst detection using the Teager-Kaiser energy operator (TKEO) in combination with digital filters for segmentation purposes. They found that the proposed method and the Wavelet decomposition have similar performance [52]. Similarly, Roldan-Vasco et al. (2018) proposed the application of the discrete Wavelet transform to reduce the detection of false negatives and to improve the signal segmentation process. In this article, the proposed method was compared together with the TKEO, obtaining an improvement in the detection of swallows [38].

Artificial intelligence techniques have been recently implemented for the automatic analysis of swallowing. Roldan-Vasco et al. (2018) proposed the automatic detection of swallowing phases of healthy subjects through the use of Artificial Neural Networks (ANN) and Support Vector Machines (SVM) considering different segments of the signal previously labeled as oral phase, pharyngeal phase, and background noise. This was applied to multichannel sEMG signals. It was found that the feature space that best describes the behavior is made up of the log-detector feature, the difference in the absolute standard deviation, the percentage of myopulse, and the mean frequency. By applying an SVM, they achieved a F1-score of 92.03 % [41].

Recently, studies on swallowing have evaluated different muscle groups individually and together, showing that sEMG can be a useful tool for the study of swallowing and dysphagia [49, 53, 42, 38, 41]. However, there are still open questions regarding the use of the technique, such as: does individual muscle evaluation allow to understand muscle dynamics in patients with dysphagia? How is the information from the different muscles involved in swallowing? Is sEMG an adequate tool for screening? [33, 39]

1.4.2. Accelerometry based cervical auscultation (ACC)

Is used to generate records of the movement of different anatomical structures of interest. The main advantage of ACC is that it is a non-invasive method, and it has a low cost; however, the sensor size and placement can be a limitation. ACC is a useful technique in the detection of movement of the cricoid cartilage during swallowing, since the hyoid bone is shifted upwards and forwards to close the airway and to generate the esophageal opening [54].

In the ACC signal acquisition, an accelerometer is placed on the cricoid cartilage parallel to the spine and perpendicular to the coronal plane [55]. Some studies use triaxial accelerometers, which allow to identify movements in the anteroposterior (AP), superior-inferior (SI), and medial-lateral (ML) axes [56, 57]. However, most studies only use sensors that allow to analyze ascent-descent and anteroposterior movements, since these are the predominant movements in swallowing (upwards and backward movement of larynx) [58, 59, 60, 61].

One of the most important aspects of studying swallowing with ACC is signal filtering. For this, different filtering methodologies have been developed for the elimination of thermal, mechanical, and electrical noise generated by the acquisition systems. Furthermore, wavelet based filters have been implemented to eliminate low-frequency noise associated with head movements [57, 62, 63, 64].

The segmentation of ACC signals, as in the sEMG signals, is based on visual analysis. The ACC signal has a high stochastic component, and its probability density function is considered to be Gaussian [61]. From this assumption, the behavior of the signal in specific segments is given by the estimation of the mean, from which a threshold is determined that allows to find large changes in the signal that are considered as swallows [65, 61].

Most of the works on ACC in swallowing focus on feature analysis that allows to describe the movement of the cricoid cartilage during swallowing, in addition to the application of classification algorithms for the detection of atypical swallows. Feature extraction methods are usually implemented in the domain of time, frequency, and time-frequency [60, 66]. For the feature extraction process, the use of empirical sliding windows has been implemented, with an usual overlap of 50% [60, 67, 68, 69, 70]. In the feature extraction of ACC signals, the studies highlight the identification of spontaneous cough, induced cough, or speech [66, 71, 72, 73, 56].

Most of the ACC related researches have been carried out at the University of Pittsburgh, where the implementation of different classification models has been proposed, for instance, the application of Linear Discriminant Analysis for the detection of abnormal swallows retrieved a sensitivity of 90.4% and a specificity of 60.0% [74]. SVM and ANN optimized

with genetic algorithms to detect swallows and cough, retrieved an accuracy greater than 99 % for the detection of cough and induced cough [72]. Bayesian classifiers, which have been used to classify aspirations in normal swallowing in people with dysphagia, achieved an accuracy of 90 % [57]. In addition, deep learning systems have been implemented seeking to track the movement of the hyoid bone using VFSS images and ACC signals, and they found that accelerometers describe correctly the trajectory of the hyoid bone [54]. Such works have implemented VFSS simultaneously with ACC [56]. However, in Colombia, the replication of this methodology has limitations due to legal restrictions for conducting invasive tests in healthy people.

The ACC is in the exploratory phase and still has open questions, such as, what incidence do age and gender have on swallowing? How do gender and age affect the appearance of signs of dysphagia? What feature extraction techniques are feasible to improve the detection of abnormal swallows? Is the evaluation of swallowing sounds from vibrations captured by accelerometers useful in research with patients with dysphagia? [60, 57, 63].

1.4.3. Multi-sensor fusion

Even though the swallowing assessment generally uses one source of information, in some cases, like in sEMG this source is represented in the acquisition of signals from several muscles simultaneously.

Considering that different anatomical structures are involved in swallowing, it is important to perform multimodal analysis instead of evaluate a single information source. Researches of multimodal analysis are limited, however, they stand out studies that integrate sEMG and bioimpedance analysis (BIA). Schultheiss et al. (2014) proposed the use of sEMG and BIA for the detection of aspirations with an SVM, considering information collected from healthy subjects and patients with swallowing disorders. They performed segmentation of the signals, obtaining an accuracy of 99.3 %, a sensitivity of 96.1 %, and specificity of 97.1 % in the classification of swallows [75].

The ACC has been also acquired in combination with acoustic signals measured by stethoscopes or microphones that capture the glottic closure [56]. However, the works developed to date have focused on the use of sound signal for segmentation processes, instead of determining the complementarity of the information provided by both sensors [59, 56].

Some algorithms have been developed for the automatic segmentation of ACC signals through neural networks considering different sources of information, particularly signals from mechanomyography and nasal cannula, showing that the use of multimodal sources in the

specific analysis ACC signal yields better results than individual analysis [67]. This leaves an open field for research on the integration of both signals [68, 63].

1.5. Problem statement

The reference techniques for the diagnosis of dysphagia are invasive, depend on the expertise of the medical staff, and have limited availability due to the cost of the equipment and the test itself. It is also difficult to follow up with patients. This is in addition to the fact that swallowing involves different neuromuscular structures and mechanical changes. Making necessary recollecting information from different sources.

Accordingly, it is necessary to evaluate non-invasive techniques that are simple to implement in clinical practice, such as electromyography and accelerometry. Although such signals have been preliminarily addressed, they have not been validated in robust and heterogeneous databases, where different causes (etiologies) of dysphagia are considered, also, they usually analyze a single dimension of swallowing, disregarding the complexity of the process in terms of anatomical structures and physiological changes.

ACC and sEMG researches of swallowing analysis, have contributed to the feature extraction, however, at present, there does not exist a consensus on the best features to describe the act of swallowing. At present, multimodal researches are few and are a broad alternative that should be explored.

1.6. Objectives

1.6.1. General objectives

To develop a methodology for integration of ACC and sEMG signals for swallowing analysis in patients with dysphagia.

1.6.2. Specific objectives

- To design a synchronous acquisition scheme for ACC and sEMG signals during swallowing tasks, for offline storage and analysis.
- To extract features of both signals in time, frequency, and time-frequency domains and to evaluate such feature spaces to obtain maximum separability between healthy individuals and dysphagic patients.

- To compare and evaluate the feature spaces and multimodal classification models to discriminate healthy and dysphagic states, by assessment of different performance measures in a database of patients with dysphagia and healthy controls.

2. Materials and methods

This chapter presents a description of the methodology implemented in the research. It describes technical aspects of the equipment and instruments used, the study population, and the steps followed to obtain the results presented in this research. Figure 2-1 shows a summary of the methodology.

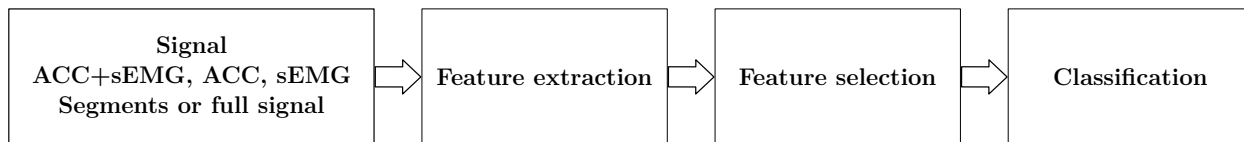


Figure 2-1. General methodology

2.1. Subjects

2.1.1. Healthy subjects

The healthy population consisted mainly of subjects with no history of dental pathologies or that modified swallowing, emphasizing that they did not present diagnosed pathologies that could give rise to dysphagia, as well as that they did not present a history of it. For this, the subjects considered healthy were evaluated using medical criteria. It was also considered the capacity to develop swallowing activities naturally.

2.1.2. Dysphagic subjects

The second group is made up of the population with dysphagia. For the conformation of this group, there was the participation of a neurologist, who, through medical criteria, and the medical history of the patients determined the person's participation in the research. In this population group, it was mainly sought that the patients presented confirmed swallowing difficulty, and that, to a large extent, they were able to follow orders.

Table 2-1 presents the inclusion and exclusion criteria of healthy and dysphagic subjects

Table 2-1. Inclusion and exclusion criteria of control and dysphagic population

	Healthy people	Dysphagic people
Inclusion criteria	Being over 18 years old.	Being over 18 years old.
	Not having a diagnosis of dysphagia.	Presence of oral or oropharyngeal dysphagia.
	Do not consume medications that modify the texture of saliva or oral secretions.	Presence of a confirmed diagnosis of central neurogenic etiology (ischemic stroke, hemorrhagic stroke, multiple sclerosis, motor neuronal disease, dementia, ECT, neuromyelitis, cerebral palsy).
	Not present central, peripheral or neuromuscular neurological pathology.	Presence of confirmed neuromuscular etiology diagnosis (inflammatory myopathies, myasthenia gravis, muscular dystrophy, neuropathy).
	Not having head and neck cancer or obstructive pulmonary disease.	
Exclusion criteria	Absence of surgical procedures in the lower 2/3 of the face or neck	
	Presence of dental pathologies.	Presence of esophageal dysphagia.
	Presence of congenital malformations in the mouth	Presence of mechanical dysphagia.
	Diagnosis or history of sicca syndrome, Sjögren's disease type.	Irradiated facial or cervical skin (under active treatment for cancer).
	Presence of active inflammatory processes inside the oral cavity.	Presence of edema or bruises at the orofacial and cervical level that prevent the application of sensors.
	Diagnosed cognitive impairment.	Recent (last three months) surgical dissection (surgical type procedure) on neck skin.
	Diagnosed cardiorespiratory compromise.	Presence of severe hypoxemia (peripheral blood oxygen saturation less than 80%). Deep brain stimulation implants.

Thirty healthy individuals and 30 dysphagic patients were recruited for train, matched by sex and age. It was determined that there is no statistical difference compared to the gender of the participants using a χ^2 test, that showed a p -value of 1. The patients were aged between 19 and 65 years and the healthy subjects between 25 and 76 years, a t -student test was applied that determined with a p -value of 0.61 that there is no statistical difference between the ages of the two population group. Likewise, a second group was selected for validation, made up of 11 healthy subjects with ages between 52 and 21 years and 11 dysphagic subjects with ages between 85 and 61 years. Table **2-2** shows the demographic data.

All patients were evaluated neurologically and phonoaudiologically to confirm their condition. The EAT-10 test was also applied, where patients with scores higher than three were selected for the study.

Table 2-2. Demographic data. The average age and deviation of each group are reported. Where: M is male, and F female

	Train			Test		
	M/F	Age of M	Age of F	M/F	Age of M	Age of F
Controls	15/15	31.60 ± 8.49	38.4 ± 14.59	5/6	35.40 ± 13.16	25.60 ± 11.13
Patients	15/15	39.90 ± 15.98	50.87 ± 12.71	6/5	69.50 ± 7.61	72.00 ± 9.11
Central neurogenic etiology						
Cerebral palsy	2/1	-	-	0/0	-	-
Cerebrovascular disease	2/1	-	-	0/2	-	-
Rubinstein-Taybi syndrome	1/0	-	-	0/0	-	-
Mitochondrial myopathy	0/1	-	-	0/0	-	-
Dermatomyositis	0/1	-	-	0/0	-	-
Cognitive disorder	0/1	-	-	0/0	-	-
Cerebellar ataxia	1/0	-	-	0/0	-	-
Traumatic brain injury	4/0	-	-	0/1	-	-
Parkinson's disease	1/0	-	-	2/2	-	-
Dementia	0/0	-	-	1/0	-	-
Neuromuscular etiology						
Muscular dystrophy	3/0	-	-	0/0	-	-
Multiple sclerosis	1/6	-	-	1/0	-	-
Amyotrophic lateral sclerosis	0/4	-	-	2/0	-	-

2.2. Data acquisition

2.2.1. Surface electromyography

The sEMG signal was recorded using the Noraxon Ultium EMG, with three EMG Sensor. This device makes it easy to acquire electromyographic signals wirelessly with M3 software and myoMUSCLE module. Table 2-3 shows the main characteristics of the Noraxon Ultium EMG. 3M 2228 Ag/AgCl surface electrodes were used with an interelectrode distance of 2 cm [40]. The signals were recorded with a sampling rate of 2 kHz and were used band-pass filters between 10-500 Hz.

Table 2-3. Main characteristics of Noraxon Ultium EMG

Specification	Value
Internal sampling resolution	24-bit
Baseline noise	< 1 μV
CMRR	<-100 dB
Input impedance	>1,000 $\text{m}\Omega$
Resolution (0 to 5,000 μV)	0.3 μV
Resolution (5,000 to 24,000 μV)	1.1 μV

2.2.2. Accelerometry

The NI-USB 6215 DAQ multifunction device from National Instruments was used to record the ACC signal. Four analog input channels were used for data acquisition (ACC and cervical auscultation) and one digital output channel for synchronization with the electromyograph. Table 2-4 shows the main characteristics of the device. The MODAC software registered with the number 13-70-441 developed by the research team was also used together with the sensor mma7362 analog sensor. This allows you to view and store signals with a sampling rate of 10 kHz, as well as stop and resume acquisition and, if necessary, use the webcam to record subjects in the swallow test.

Table 2-4. NI-USB 6215 DAQ Multifunction device highlights

Feature	Value
Bus connector	USB 2.0
Analog inputs	16
Differential analog inputs	8
Maximum sampling rate	250 kS/s
Analog input resolution	16 bits
Absolute accuracy analog input	2690 μ V
Analog input impedance	60 V Channel-to-ground insulation

2.2.3. Synchronization

Considering that the signals were acquired using two independent devices, a synchronization strategy was implemented. The synchronization process consists of the generation of a digital pulse in the MODAC software. This is saved together with the ACC signals. The digital pulse is recorded by the Noraxon Ultium EMG, and it is stored with sEMG signals in the M3 software. Synchronization was achieved by aligning the pulses of both registers offline (see Figure 2-2).

The initial pulse marks the beginning of the swallowing task. It is important to bear in mind that it was sought to have segments of background noise between each of the tasks. In the same way, a second pulse would be in charge of marking the end of the swallowing activity.

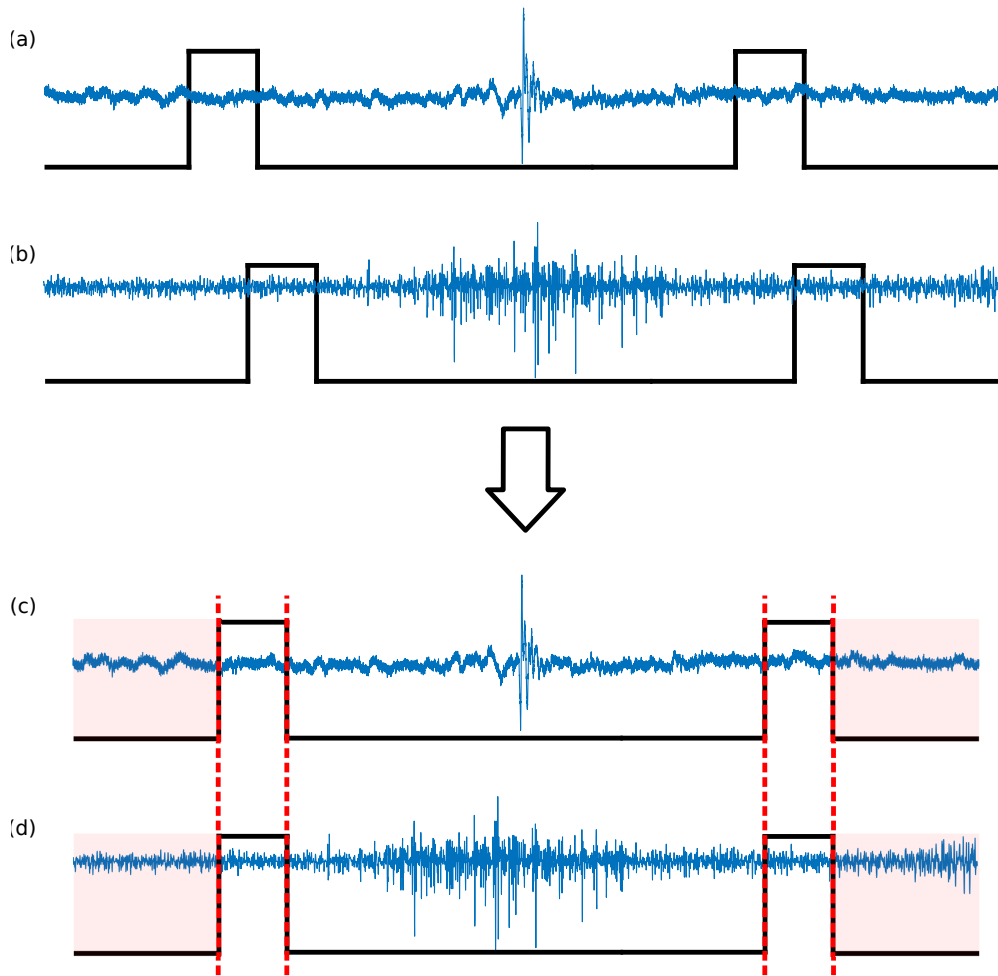


Figure 2-2. Synchronization diagram by means of pulses in the ACC and sEMG signals. Where (a) is the ACC signals with the synchronization pulse, (b) is the sEMG signals with their respective synchronization pulse, and (c) and (d) are both signals synchronized through the pulses

2.2.4. Signal recording

The implemented protocol consisted of supplying three different volumes and two consistencies of liquids. Included 5, 10, and 20 mL of water and yogurt, in addition to a dry swallow (W5, W10, W20, Y5, Y10, Y20, and S) following the order that can be seen in the Figure 2-3



Figure 2-3. Acquisition protocol for ACC and sEMG signals.

The evaluated subjects were placed in an upright sitting position. Pairs of Ag/AgCl elec-

trodes were placed in a differential configuration. These were placed in the right and left suprahyoid muscles, as well as in the right infrahyoid muscle, leaving the left infrahyoid free for the accommodation of the accelerometer. The accelerometer was placed in the cricoid cartilage, parallel to the cervical spine, perpendicular to the coronal plane. Figure 2-4 shows the general diagram of their location.

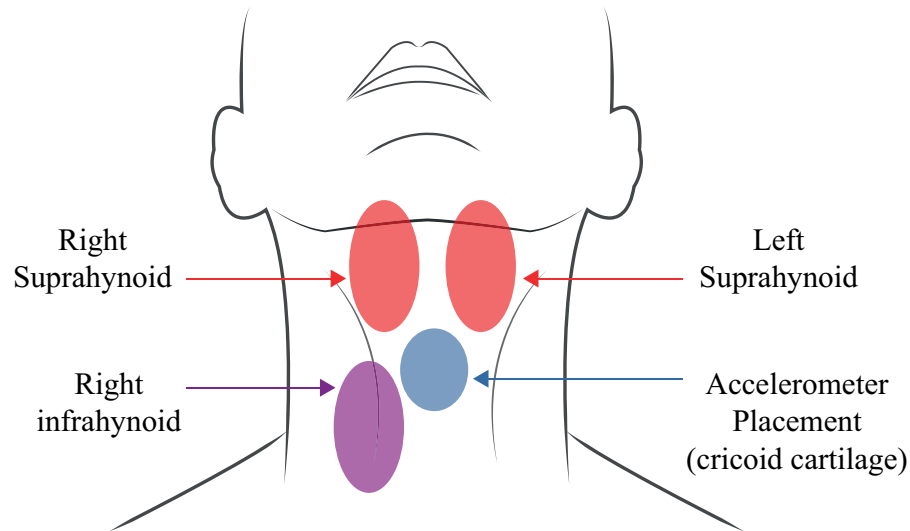


Figure 2-4. Location of sEMG electrodes and accelerometer for data collection.

In some cases, it was not possible to record all swallowing tasks of the subjects studied, for safety purposes. Table 2-5 shows the number of signals available per swallowing task in each of the population groups.

Table 2-5. Number of analyzed boluses per population group

	W5	W10	W20	S	Y5	Y10	Y20
Controls	30	29	27	30	30	30	30
Patients	28	26	22	28	29	27	25
Total	58	55	49	58	59	57	55

2.3. Pre-processing

A four-stage filtering scheme was applied. It was implemented a filter for detrend, a notch filter at 60 Hz, as well as band pass filters, and wavelet denoising was applied for ACC and sEMG signals. The parameters of each signal are presented below.

2.3.1. ACC pre-processing

The filtering of the ACC signal was carried out with a band-pass filter between 0.1-3000 Hz, and the best parameters for the implementation of wavelet denoising were explored.

Wavelet denoising

Wavelet denoising is a filtering technique for the elimination of high-frequency noise. The technique decomposes the signal into bands containing noise information, obtaining the wavelet coefficients. These coefficients are modified by a threshold, that allows the reconstruction of the filtered signal. The assumption of Gaussianity is a constraint. This method is based on the discrete wavelet. The following parameters must be optimized:

- The mother wavelet that will be used to perform the decomposition. The following wavelets were assessed: Coiflets (coif2 to coif5), Daubechies (db2 to db9) and Symlets (sym3 to sym6).
- Decomposition levels: Number of information bands to analyze, in this case, from 2 to 9.
- Threshold selection rule (TPTR): Determines the rule for threshold selection. Where *rigsure* uses a quadratic loss function for the soft threshold estimator, *sqtwolog* uses a universal threshold defined as $\sqrt{2 \ln(\text{length}(x))}$, *heursure* uses a mix of the above methods, considering the signal-to-noise ratio (SNR), and *minimaxi* uses a fixed threshold.
- Type of thresholding (SORH): soft thresholding (*s*), hard thresholding (*h*). Where the hard threshold sets the values below the threshold to 0, while the soft threshold sets the same values to 0, but additionally subtracts the threshold from the values that exceed it [76].
- Multiplicative threshold rescaling (SCAL): no rescaling (*one*), is the basic model; rescaling using a single estimation of level noise based on first-level coefficients (*sln*), changes the scale by a single noise estimate from the first level coefficients; rescaling using a level-dependent estimation of level noise (*mln*), scales by level-dependent noise estimation.

For the application of this filtering step, in ACC signals, strange artifacts were identified and background noise segments, that would not be part of swallowing. They were also identified swallowing segments. Which were obtained by manual segmentation (see Figure 2-5). Different parameters were evaluated for the elimination of noise in each segment obtained. The spectrogram of each of the segments was calculated, averaged, and used to compute the

SNR. The optimal parameters to filter the ACC signal were determined to maximize the SNR.

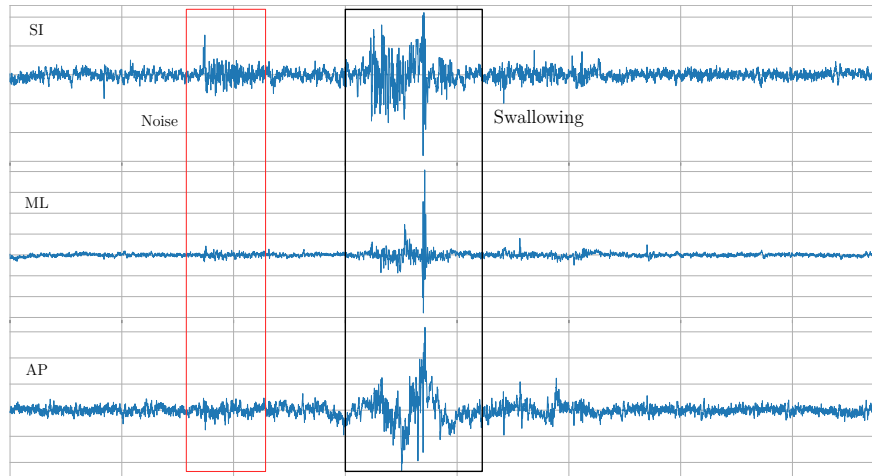


Figure 2-5. Typical ACC signal. Noise and swallowing events are highlighted

2.3.2. EMG pre-processing

In the sEMG signals, the band-pass filter was applied between 25 and 450 Hz in combination with wavelet denoising with a Daubechies 5 mother wavelet (db5) with five decomposition levels, parameters reported in previous researches [52].

2.4. Feature extraction

It consists of mathematically determining the behavior of the signals. Feature extraction processes are usually implemented in the time, frequency, and time-frequency domains, as well as information-theoretic features.

2.4.1. Time domain

It consists of obtaining descriptors that represent the behavior of a certain signal over time. This method provides information on the morphology and complexity of the signal. The characteristics calculated in this domain are sensitive to noise, so it is necessary to implement filtering techniques [77], however, its calculation is simple and of low computational cost. The table 2-6 shows the features in the time domain that were used.

Table 2-6. Time domain features. Abbreviations: n is the number of points evaluated; s_i : i -th element of the vector; \bar{x} : mean of the vector; ϵ : amplitude threshold

Feature	Description	Equation
Variance	The variance is the second statistical moment, represent how far the data is from the mean [78].	$\sigma_n^2 = \frac{1}{n} \sum_{i=1}^n (s_i - \bar{x})^2$
Root Mean Square	It is a measure of amplitude and estimates the energy content in the signal. It is used to calculate the mean in data sets that take negative values [78].	$RMS = \sqrt{\frac{1}{n} \sum_{i=1}^n s_i^2}$
Integral	Index to detect muscle activity [79].	$integral = \sum_{i=1}^n s_i $
Wavelength	Calculate the complexity of the different wave segments [80].	$WL = \sum_{i=1}^{n-1} s_{i+1} - s_i $
Difference absolute standard deviation value	Calculates the RMS of the wavelength [81].	$DASDV = \sqrt{\frac{1}{n-1} \sum_{i=1}^{n-1} (s_{i+1} - s_i)^2}$
Zero-Crossing	Indicates the number of times that the signal goes through 0 and changes the sign. In some cases used a threshold, and indicates the number of times the signal goes through [78].	$ZC = \sum_{i=1}^{N-1} (s_i \times s_{i+1} < 0) \cap \epsilon (s_i - s_{i+1})$
Willison amplitude	Calculates the number of times the absolute value of two consecutive samples exceeds a threshold [78].	$WAMP = \sum_{i=1}^n f(s_i - s_{i+1})$ $f(x) = \begin{cases} 1, & s \geq \epsilon \\ 0, & \text{in any other case} \end{cases}$
Myopulse percentage rate	It is calculated assigning values of 1 when the absolute value of the signal exceeds a threshold ϵ , used mainly in sEMG [82].	$MYOP = \frac{1}{n} \sum_{i=1}^n [f(s_i)]$ $f(s) = \begin{cases} 1, & s \geq \epsilon \\ 0, & \text{in any other case} \end{cases}$
Teager-Kaiser	The Teager-Kaiser energy operator quantifies rapid energy changes in signals with a single frequency variable in time.	$TKEO = s_i^2 - s_{i+1}s_{i-1}$
LOG Detector	It is an indicator of the force with which a muscle is activated [78].	$LOG = \exp\left(\frac{1}{N} \sum_{i=1}^N \log(s_i)\right)$

The implemented threshold was defined by $\epsilon = \text{mean} + h \times \text{std}$ calculated in the first 50 ms, where h was 3 for the sEMG signals, and 1.2 for ACC, the latter taking into account that previously thresholds of 2.5 have been reported, however, the use of half of this gave better results [83, 84]

2.4.2. Frequency domain

It is implemented to determine specific changes in the frequency components of the signals or time series. To do this, tools such as Fast Fourier Transform (FFT) are used, which allows a signal to be broken down into its frequency components. Table 2-7 shows the features used in the frequency domain.

Table 2-7. Frequency domain features. Abbreviations: f_i : frequency of the spectrum in i ; M : size of the power spectral density P_j : power spectrum; ULC : upper-cutoff frequency of the low frequency band; LLC : lower-cutoff frequency of the low frequency band; UHC : upper-cutoff frequency of the high frequency band; LHC : lower-cutoff frequency of the high frequency band. Definitions are taken from [78]

Feature	Description	Equation
Frequency ratio	Calculates the relationship between the low-frequency and high-frequency components.	$FR = \sum_{j=LLC}^{ULC} P_j / \sum_{j=LHC}^{UHC} P_j$
Mean power	Calculates the mean power of the power spectrum of the analyzed signal.	$MNP = \sum_{j=1}^M P_j / M$
Mean frequency	Calculate the average of the frequencies present in a signal.	$MNF = \sum_{j=1}^M f_j P_j / \sum_{j=1}^M P_j$
Median frequency	Divides the spectrum into two regions with equal amplitude.	$MDF = \frac{1}{2} \sum_{j=1}^M P_j$
Peak frequency	It is the maximum frequency found.	$PKF = \max\{P_j\}, \quad j = 1, \dots, M$

2.4.3. Time-frequency domain

The representation of signals in time-frequency allows us to understand their behavior in both domains. transformation techniques such as the Short-Time Fourier Transform (STFT) or the wavelet transform are implemented for its analysis. Table 2-8 shows the calculated time-frequency features.

Table 2-8. Time-frequency features. Abbreviations: DL : number of decomposition levels; E_{ADL} : relative energy of the final approximation coefficient: j -th relative energy of the j -th detail coefficient.

Features	Description	Equation
Wavelet energy	Evaluates the energy contained in different scale ranges [85].	$E_T = \frac{1}{100} \left(E_{ADL} + \sum_{j=1}^{DL} E_{Dj} \right)$
Wavelet entropy	Gives information on the degree of disorder in which the signal is found [86].	$W_{ent} = -E_T \log_2 E_T$

2.4.4. Information-theoretic features

They are features that allow you to have information about the regularity and complexity of the data. For this case, the discrete-time series is required to change to its phase state. The phase state is represented as follows:

$$\mathbf{X}_m(i) = [x_i \ x_{i+\tau} \ \cdots \ x_{i+(m-1)\tau}] \quad (2-1)$$

Where $\mathbf{X}_m(i)$ is the state of the system at the discrete-time i , x_i is the i -th sample of the signal, τ is the reconstruction delay and m is the embedding dimension [87]. The embedded space is used to compute the sample entropy and the Largest Lyapunov exponent. Table 2-9 shows the Information-theoretic features used in this work.

Table 2-9. Non-linear features. Abbreviations: r : tolerance for accepting matches (when the distance between two trajectories is smaller than r); $A^m(r)$ and $B^m(r)$: probabilities that two trajectories will match for $m + 1$; m : points; n : is the algorithm iteration; k : number of blocks into which the signal is broken down; $f(s_n)$: iterated mapping s_{n+1} ; n : is the algorithm iteration.

Features	Description	Equation
Sample entropy	It is a measure used to evaluate the temporal complexity of signals, generally physiological. The SampEnt defines a tolerance (r) for accepting matches (if the distance between two trajectories is smaller than r), and $A^m(r)$ and $B^m(r)$ are the probabilities that two trajectories match for $m + 1$ and m points, respectively [88].	$\text{SampEn}(m, r) = \lim_{N \rightarrow \infty} \left[-\ln \frac{A^m(r)}{B^m(r)} \right]$
Lempel-Ziv Complexity	Is extracted by computation of the complex envelope of the signal. Afterward, such an envelope is binarized by thresholding. Finally, the count of different binary patterns is carried out [89].	$LZC = \frac{k \log_{100} n}{n}$
Largest Lyapunov exponent	It is a measure of dynamic systems, which characterizes the separation rate infinitesimally close trajectories [87]	$\lambda(x_0) = \lim_{n \rightarrow \infty} \frac{1}{n} \sum_{i=0}^{n-1} \ln f'(s_i) $

2.4.5. Statistical moments and signal segmentation for the feature extraction

The feature extraction process returns features that represent the behavior of the signal in each of the domains analyzed. The feature extraction of ACC and sEMG signals was performed by the implementation of a sliding window scheme with overlap (see Figure 2-6). From this process, each feature is represented by a vector is obtained. The length of such vector (N_f) depends on the length of the original signal (N), the size of the window (N_w), and the step size (Δ), follows:

$$N_f = \frac{N - N_w}{\Delta} + 1 \quad (2-2)$$

The parameters used for the implementation of the sliding window were frames of 100 and 250 ms for ACC and sEMG respectively, with 50% overlap. Information-theoretic features were not extracted from sEMG signals due to window size restrictions.

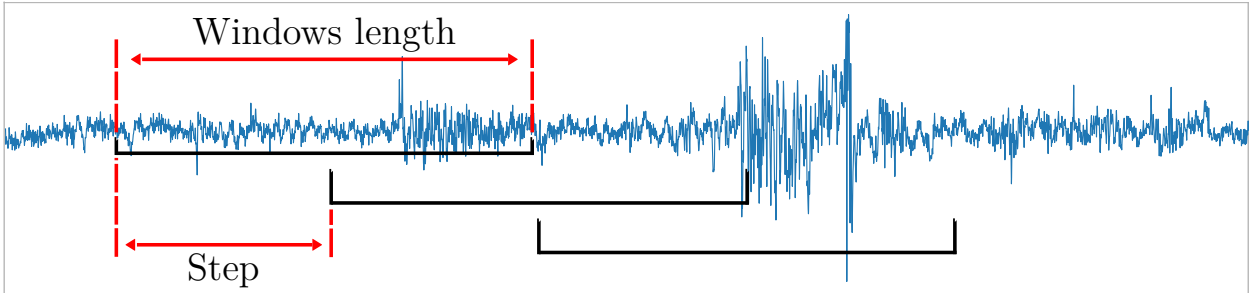


Figure 2-6. Sliding window in ACC signals.

To obtain numerical values that represent the behavior of the vector obtained from the sliding window, each of the first four statistical moments, the maximum and minimum are usually calculated, thus obtaining six features per feature vector. The corresponding equation for each of the four moments is presented below.

- Mean (μ)

$$\mu = \frac{1}{n} \sum_{i=1}^n s_i \quad (2-3)$$

- Variance ($VAR(S)$)

$$\text{Var}(S) = \frac{1}{n} \sum_{i=1}^n (s_i - \mu)^2 \quad (2-4)$$

- Skewness (γ)

$$\gamma = \frac{\mu_3}{\sigma^3} \quad (2-5)$$

where μ_3 is the third moment around the mean and σ is the standard deviation

- Kurtosis (β)

$$\beta = \frac{\mu_4}{\sigma^4} \quad (2-6)$$

where μ_4 is the fourth central moment.

The feature extraction was performed using different signal lengths. It was used the full signal, and segments of 1000, 750, and 500 ms. The segmentation consisted of the identification of the swallowing center, it was used SI channel for reference, and open windows of half the desired signal time on each side (see Figure 2-7). Each segment, as well as the full signal, were evaluated by means of the previously exposed methodology (sliding window and calculation of the first four statistical moments and the minimum and maximum). When fixed-size signal segments were used for feature extraction (1 s, 750 ms, and 500 ms), the segments outside these times were discarded for the to feature extraction processes. With this process, it was sought to determine the optimal window size for the analysis of the swallowing tasks.

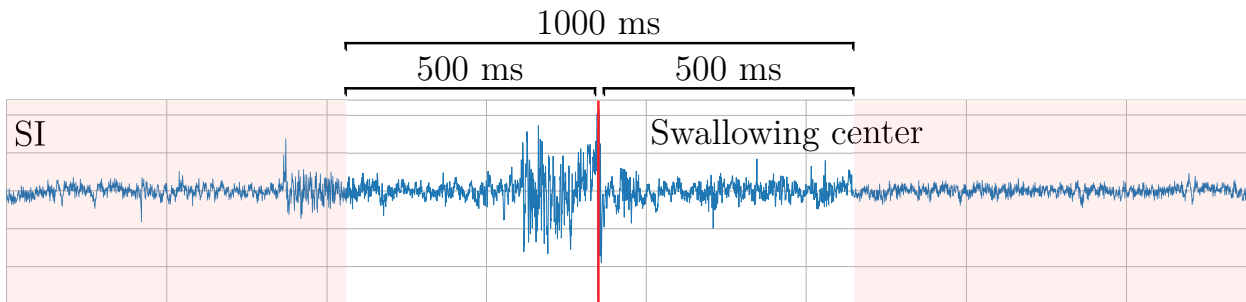


Figure 2-7. Segmentation example for a 1000 ms window from the superior-inferior channel. Red areas were discarded or were disregarded for feature extraction.

It is important to note that the swallowing tasks were analyzed individually, obtaining one feature space for each task, which would be made up of ACC and sEMG features, a process known as “early fusion”. Figure 2-8 shows a summary of the process described above.

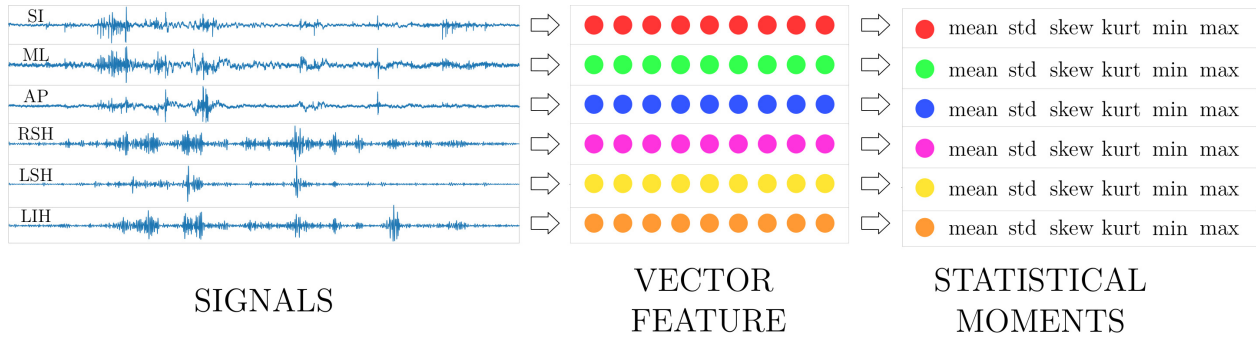


Figure 2-8. Graphical representation of feature extraction scheme.

2.5. Feature selection

Feature extraction processes ease the interpretation of the phenomenon under study. However, not all the features describe the phenomenon correctly. Thus, it is recommended to implement feature selection methods, considering, that to a large extent the classification results depend on the use of the appropriate features.

Filtering methods for feature selection depend on statistical scores that relate the feature to the classes. As an advantage, they do not depend on the classification algorithm [90]. Below is a description of the methods used.

Based on Principal Component Analysis method (PCA)

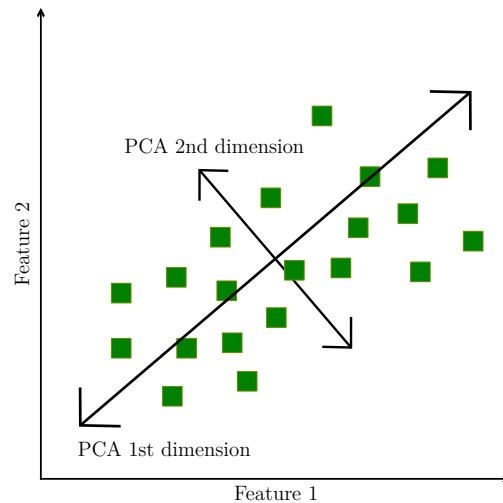


Figure 2-9. Graphical representation of principal components analysis

It is a technique widely used and applied to different fields. Through this technique the representation of feature spaces is sought from the main components of the vectors that make up the feature space (see figure **2-9**). Although in the strict sense this is not a feature selection method, it can be used as such from the score of the variance of the vectors of the original feature space [91, 92].

The method finds new features spaces from the normalized linear combination of each of the features (X_1, X_2, \dots, X_p) of the original set, thus:

$$Z_1 = \phi_{11}X_1 + \phi_{21}X_2 + \dots + \phi_{p1}X_p \quad (2-7)$$

The ϕ defines the component, representing the directions of the maximum variance of the vectors. ϕ can be interpreted as the importance of each of the variables as a function of their covariance and can be used to score each of the variables in the input set. The fact that the linear combination is normalized implies that:

$$\sum_{j=1}^p \phi_{j1}^2 = 1 \quad (2-8)$$

Minimum Redundancy - Maximum Relevance (mRMR)

The method seeks to identify the relevance of each of the characteristics calculated with respect to a target variable or label. The features are considered good if they present a degree of balance in their relevance and redundancy, seeking maximum relevance and minimum redundancy [93].

Using the mutual information (MI) of the features, which, unlike the correlation coefficient that only evaluates linear dependencies, the MI can find linear and non-linear dependencies, the mRMR determines which features can be eliminated (see Figure **2-10**) [94].

The mRMR criterion combines the equations of max-relevance (D), where characteristics that are considered relevant to the classification problem are selected (Equation 2-10) and the min-redundancy (R), considering that the features selected may contain redundant information (Equation 2-11) to solve an optimization problem as can be seen in Equation 2-12

$$I(x; y) = \sum_{y \in Y} \sum_{x \in X} p_{(x,y)}(x, y) \log \frac{p_{(x,y)}(x, y)}{p_{(x)}(x)p_{(y)}(y)} \quad (2-9)$$

$$\max D(S, c), \quad D = \frac{1}{|S|} \sum_{s_i \in S} I(x_i; c) \quad (2-10)$$

$$\min R(S), \quad R = \frac{1}{|S|^2} \sum_{x_i, x_j \in S} I(x_i, x_j) \quad (2-11)$$

$$\max \Phi(D, R), \quad \Phi = D - R \quad (2-12)$$

Where I is the mutual information, (x, y) are random variables, $p(x), p(y), p(x, y)$ are probability density functions, x_i are the individual features, c is the class, S is the feature set with m features

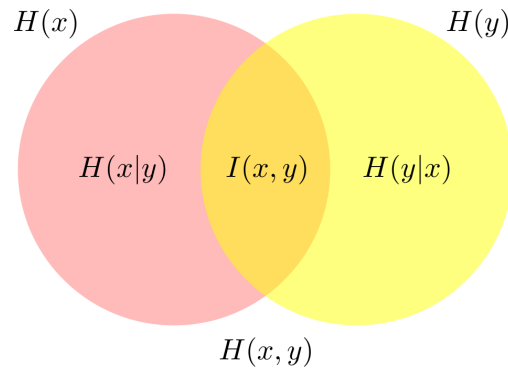


Figure 2-10. Graphical representation of the mutual information $I(x, y)$. H denotes the entropy of the random variables x or y .

Receiver Operating Characteristic (ROC) curve

The use of the ROC curves for the feature selection consists of calculating the area under the curve (AUC) that each one of the features, keeping in mind the classes. This technique is easy to apply and is widely used when dealing with bi-class problems. To find the features to be used, a threshold is determined based on the AUC that must be exceeded. Figure 2-11 shows the area under the curve of six different characteristics in a bi-class classification problem. To calculate the AUC, the rate of true positives and false positives is considered, which are described in Section 2.6.3.

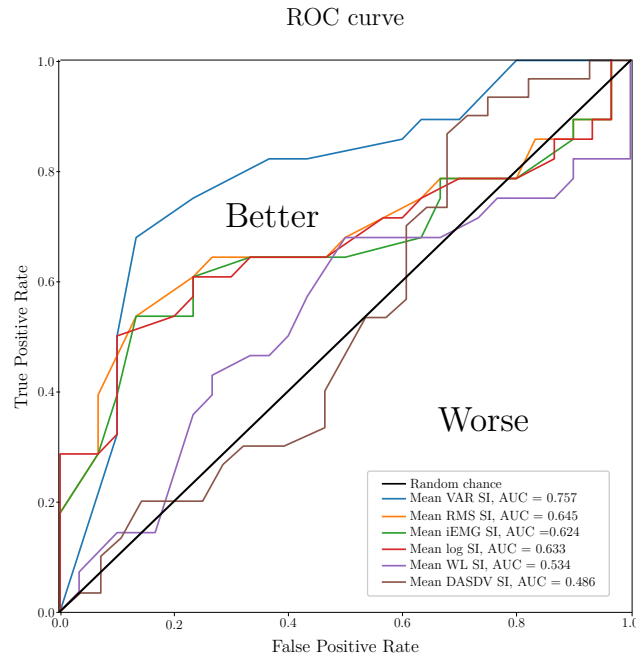


Figure 2-11. ROC curve of six different features in a classification problem

The feature selection consisted of the implementation of the filter methods described above, which allow reducing the feature spaces without reliance on a classifier. Furthermore, one feature space per individual domain was considered for analysis.

Three classification scenarios were considered: one using only ACC signals; another with sEMG only; and finally, another with the combination of both sources of information.

- ROC: Features with an AUC greater than 0.6, 0.7 and 0.8 were extracted (ROC 0.6, ROC 0.7 and ROC 0.8).
- PCA: Select the components so that the variance found is greater than 0.8
- mRMR: The number of characteristics was selected automatically taking into account the mutual information regarding the label.

2.6. Classification and optimization

2.6.1. Classification

In the Machine Learning field, it is possible to find algorithms that allow determining the membership of the data to one of the classes. This process is known as classification, it can be bi-class, or multi-class, depending on the number of possible outputs of the algorithm. The methods implemented in this work are listed below.

Support Vector Machines

Are algorithms used in classification and regression problems. In the case of classification, SVM's are designed mainly for bi-class problems, however, they can also be applied to multi-class problems [95].

The SVM algorithm estimates hyperplanes where the support vectors can be located and the classes are separated, looking for each of the classes to be located on each side of the hyperplane. This is accomplished by $y_i (w \cdot x_i + b) \geq 1$ $i = 1, \dots, N$; where N is the number of data, x_i is the training set, y_i is the class, and w and b are parameters that satisfy the algorithm. However, linear separability is not always possible, so the classification problem turns into:

$$y_i(w \cdot x_i + b) \geq 1 - \xi_i \quad i = 1, \dots, N \quad (2-13)$$

where $\xi_i \geq 0$ allows points that have been misclassified. Finally, the SVM classification problem is sought to be solved through the optimization that is given by:

$$\begin{aligned} & \min_{w,b,\zeta} \frac{1}{2} w^T w + C \sum_{i=1}^n \zeta_i \\ & \text{subject to } y_i (w^T \phi(x_i) + b) \geq 1 - \zeta_i \\ & \zeta_i \geq 0, i = 1, \dots, n \end{aligned} \quad (2-14)$$

To solve this problem, the aim is to maximize the margin, with a penalization when a sample is poorly classified or within or at the limit of the margin. Ideally we have that $y_i (w^T \phi(x_i) + b) \geq 1$ in perfectly separable problems, but this is not always possible, for which allows some samples to be at a distance ζ_i from the margin. In addition, the training data is mapped in a higher-dimensional space defined by the function ϕ .

Normally, the problems to be solved by means of SVM's do not have linear behaviors and have more than two features. To solve this problem, the features are projected to a space of greater dimensionality that favors the separation of classes. This is achieved by kernel functions.

In Figure 2-12 it is possible to see a general diagram of the support vectors and the hyperplane, where it is observed that the method uses the samples that are closest to the margin, which contributes to the decrease in the cost of the algorithm.

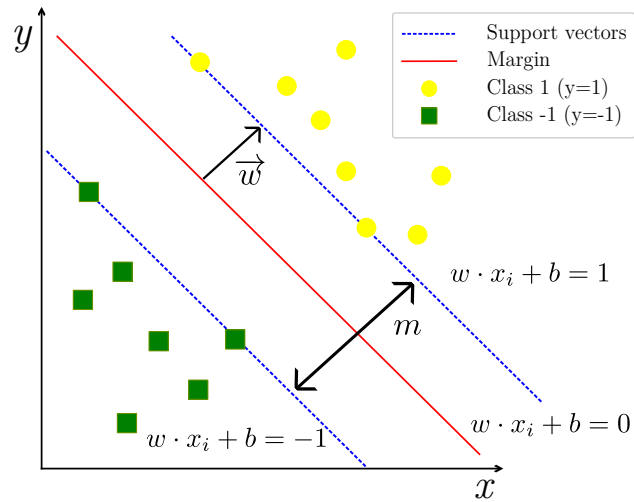


Figure 2-12. Graphical representation of the support vectors and the separation hyperplane

Multilayer perceptron (MLP)

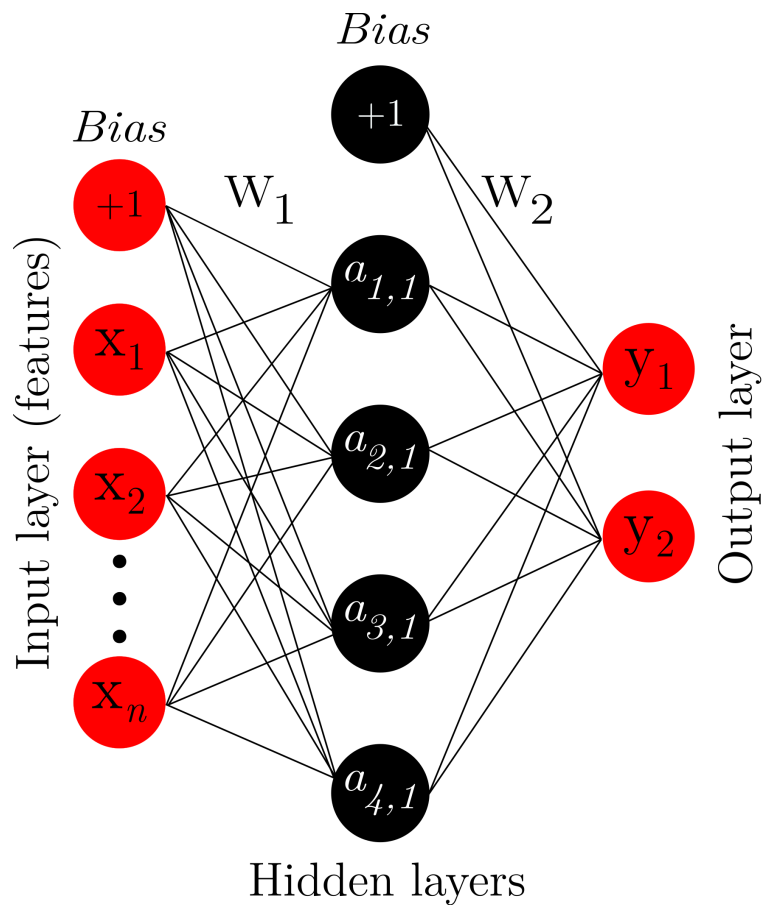


Figure 2-13. Representation of a neural network with one hidden layer

It is a supervised machine learning model where, from input sets, that are located in what is known as input layers, and by performing weighted sums and applying a non-linear activation function between layers (see Equation 2-15), the probability is obtained of belonging to one class or another. In Figure 2-13 there is a graphic representation of an MLP. MLP, unlike logistic regression models, can have hidden layers with different activation functions. The calculation is carried out in three steps, the initial one where the output of the previous neuron is multiplied by its weight, in the second step the weighted sum is performed, and finally, the activation function is applied [96], Figure 2-14 shows each of the steps that are carried out internally in neurons. In bi-class problems, a sigmoid function is usually implemented in the last layer, since it works especially well in classification problems.

$$u_i = \sum_{i=1}^m (w_i \cdot x_i) + b \quad y_1 = f(u_i) \quad (2-15)$$

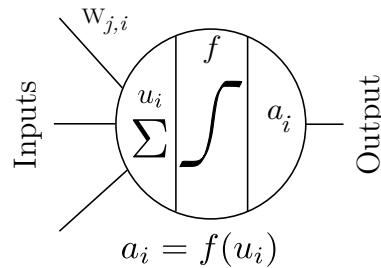


Figure 2-14. Neuron structure

Where w are the weights, x the output of the previous layer neuron, b is the bias, and $f(u_i)$ is the non-linear activation function. There are different activation functions that can be implemented in MLP models, below are the formulas of some of them.

- Rectified linear unit function (ReLU)

$$f(x) = \max(0, x) \quad (2-16)$$

Where x is the input to the neuron

- Hyperbolic tangent activation function (tanh)

$$f(x) = \tanh(x) \quad (2-17)$$

- Logistic sigmoid function:

$$\sigma(x) = \frac{1}{1 + e^{-x}} \quad (2-18)$$

Extreme Gradient Boosting (XG Boost)

It is a machine learning method where several decision trees are trained, each of them depends on the residual δ and on the previous tree. In addition to, a cost function that seeks to minimize the error of each of the trees. In each iteration, the algorithm optimizes the XG Boost and minimizes the prediction error. The predictions in the algorithm iterations are calculated like this: $\hat{y}_i^{(k)} = \hat{y}_i^{(k-1)} + f_k(x_i)$. And the output of the algorithm is determined by the weighted sum of each of its trees [97], as can be seen in the formula below.

$$\hat{y}_i = \sum_{k=1}^K f_k(x_i), f_k \in \mathcal{F} \quad (2-19)$$

Where \mathcal{F} is the function spaces of each of the trained trees, and k denotes the number of trained trees. It is important to consider that the decision trees produce a continuous variable as an output, so the classification depends on the probability function given by $p(y_i = 1 | x_i) = \sigma(\hat{y}_i(x_i))$ where σ is the sigmoid function. Figure 2-15 is a graphical representation of the XG Boost model.

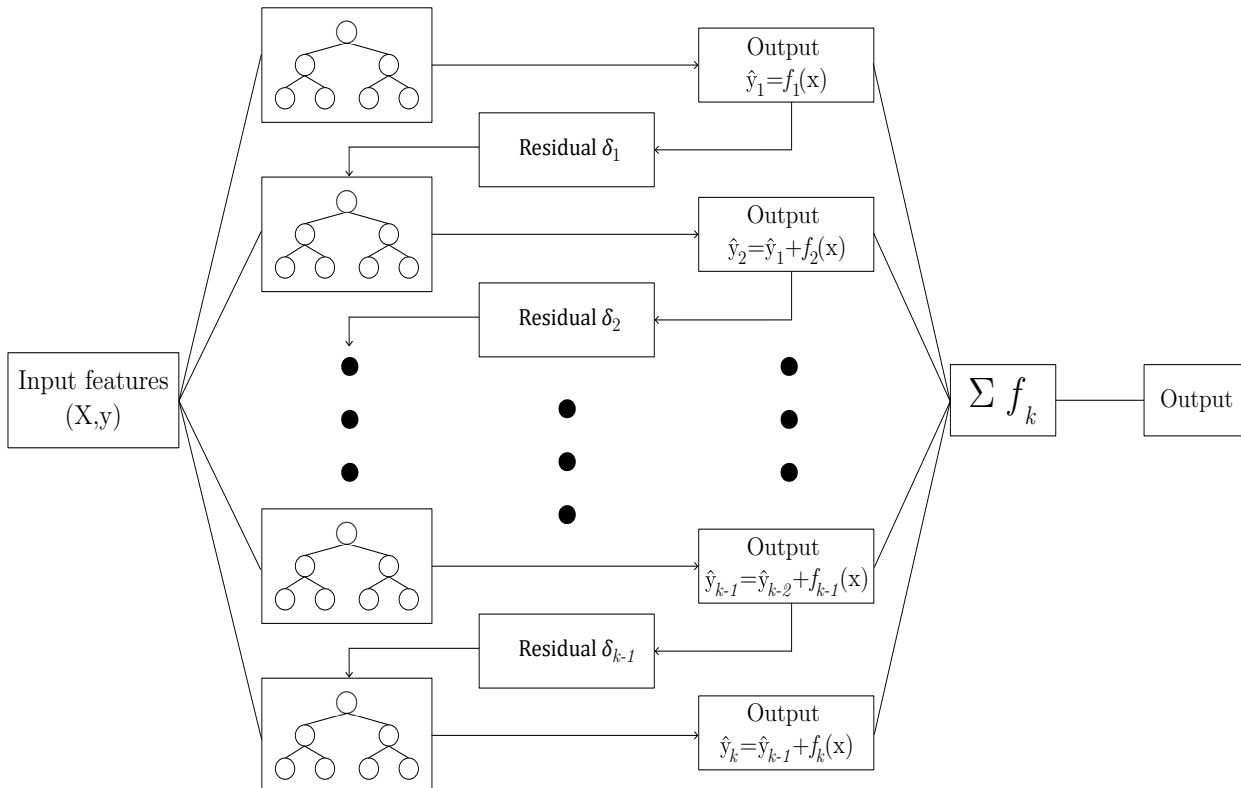


Figure 2-15. XGBoost graphical representation

***k*-nearest neighbors (KNN)**

The algorithm finds the closest neighbors of the sample to be classified. The algorithm calculates the distance between this point and the k points that are part of the set of training, and calculates the mode of the classes of each of the closest points. According to this mode, the class to which the new point belongs is determined. The main recommendation is to use odd k in order to avoid bi-mode problems (see Figure 2-16). There are different methods for calculating the distance, below is the mathematical formulation of Euclidean distance, the method used in this work:

$$d(p, q) = \sqrt{\sum_{i=1}^n (p_i - q_i)^2} \quad (2-20)$$

Where p_n and q_n are Cartesian coordinates in n -dimensional Euclidean space

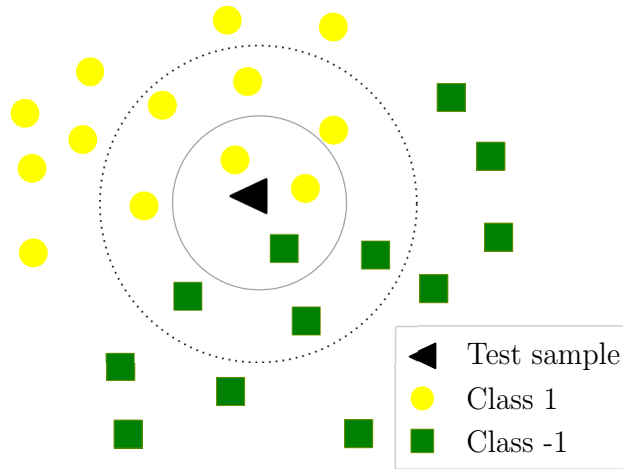


Figure 2-16. KNN graphical representation

2.6.2. Optimization

The algorithms of feature selection, machine learning, and deep learning include different parameters and hyperparameters, the best selection in these aspects entails the generation of the best results. Various methods have been created that seek the choice of the best hyperparameters, such as the grid search. This method consists of determining the parameters under which the algorithm that we want to optimize will work, and under the grid search scheme, all possible combinations of these defined parameters are evaluated, seeking to maximize or minimize a metric defined from the beginning [98].

Stratified cross-validation with 10 outer and 5 inner partitions was performed for four different classifiers. For each of them, a grid-search was implemented with the AUC as an optimization criterion, and the F1-score, accuracy, precision, and sensitivity were also calculated. The parameters optimized for the grid search are described below.

- SVM: Kernel: Radial basis function, sigmoid and linear. C: 10^{-4} to 10^4 . γ : 10^{-4} to 10^{-4} .
- MLP: Solver: Adam and stochastic gradient descent. Learning rate (α): 10^{-4} to 10^4 . Hidden layers: (10,1), (10, 10), (10, 50), (50,), (50, 10), (50, 50), (50, 100), (100,1), (100, 50), (100, 100). Activation functions: ReLU, tanh, and logistic
- XG Boost: Depth of tree: 2, 5, 10, 20, 30, 50 and 100. Weights Balance: 1, 10, 25, 50, 75, 99, 100 and 1000.
- KNN: Neighbors: 3, 5, and 7.

2.6.3. Model selection

In the classification processes, performance measures were determined to identify the rate of successes or failures of the classifier. The confusion matrix shows the true-positive (TP), false-positive (FP), true-negative (TN), and false-negative (FN). Figure 2-17 shows how a confusion matrix is presented.

		True class	
		Positive	Negative
Predicted class	Positive	True Positives TP	False Positives FP
	Negative	False Negatives FN	True Negatives TN

Figure 2-17. Structure of matrix confusion

The TP, FP, FN, and TN, allow to evaluate of the performance of the proposed algorithm by different metrics, as described below:

- Precision: it is the ratio of true positives among all true results

$$Precision = \frac{TP}{TP + FP} \quad (2-21)$$

- Sensitivity: seeks to find the proportion of true positives that were correctly identified

$$Sensitivity = \frac{TP}{TP + FN} \quad (2-22)$$

- F_1 score: it is the measure of precision that a test has, it combines the precision and completeness values of the results of an algorithm.

$$F_1 score = 2 \times \frac{Precision \times Sensitivity}{Precision + Sensitivity} \quad (2-23)$$

- Accuracy: It is the proportion of true results among the total of cases examines

$$Accuracy = \frac{TP + TN}{TP + TN + FP + FN} \quad (2-24)$$

- ROC-AUC: Its definition is found in Section 2.5. In this case, is calculated to determine the performance of the implemented classification algorithms

Once the results of the implemented classifiers were obtained and evaluated, the models that presented the highest AUC were chosen per swallowing task. If two models, retrieved the same AUC, the best one was selected as the one with the highest sensitivity. The most common combination of hyperparameters found in each partition of the selected models was selected, seeking to evaluate the models again.

Figure 2-18 illustrates the summary of the methodology.

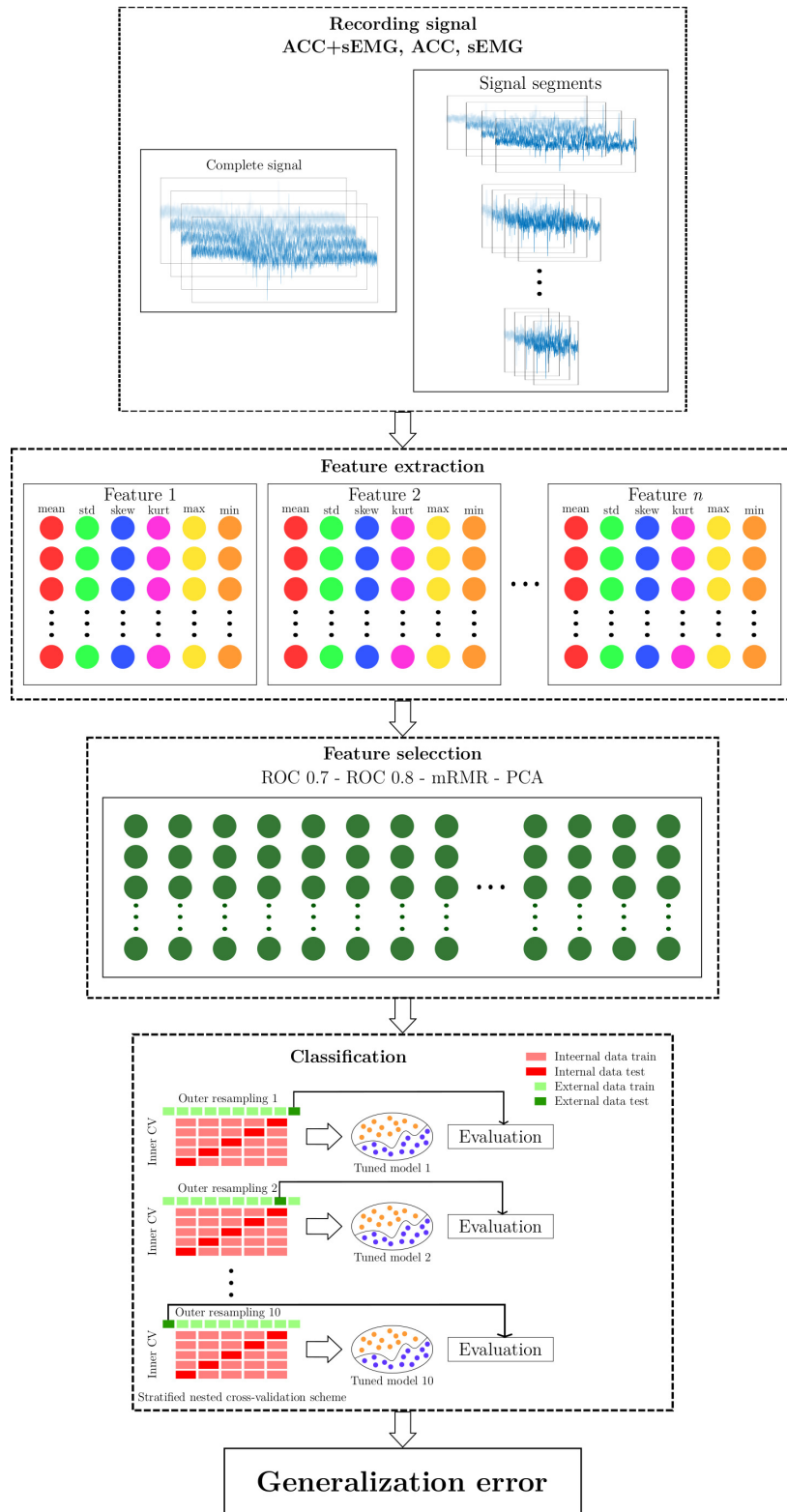


Figure 2-18. Methodological flowchart.

3. Results

3.1. Acquisition of ACC signal

3.1.1. Custom software MODAC

According to the design requirements established by the research team, software called MODAC was developed, which allows the capture of ACC signals, and cervical auscultation, the visualization of signals in real-time, and storage for offline analysis. The software was tested by researchers and used in healthy and pathological subjects.

The main features of the designed software are provided next.

Main window



Figure 3-1. MODAC main window

The software incorporates a module for the acquisition of ACC signals synchronously with video images. Also, a module for the acquisition of ACC and cervical auscultation signals. In the same way, a module was incorporated that allows, using impulses, the segmentation of the sEMG signals. Figure 3-1 shows the main window of the designed software.

Synchronization

The synchronization tool consists of a digital button on the MODAC. In this case, the digital button is in charge of generating the impulse that is stored in the MODAC and sent through the NI-USB 6215 DAQ to the Noraxon.

sEMG segmentation

The MODAC incorporates a module of pulse generation that allows having an indicator of the onset and offset of the sEMG signal. This is useful as it allows the segmentation of swallowing tasks offline for further analysis. Figure 3-2 shows the design of this module. In this module, the user has the Start button, which allows generating a new file with the name of the subject evaluated. It also has two buttons that allow to pause, resume and end the process, and a button that sends the segmentation pulse for the sEMG signals.



Figure 3-2. Synchronización module

ACC acquisition

The MODAC main module allows the acquisition of ACC and cervical auscultation signals. It also allows the generation of pulses for the synchronization and segmentation of offline signals. Figure 3-3 shows the functioning of MODAC software were the ACC acquisition and performed cervical auscultation.

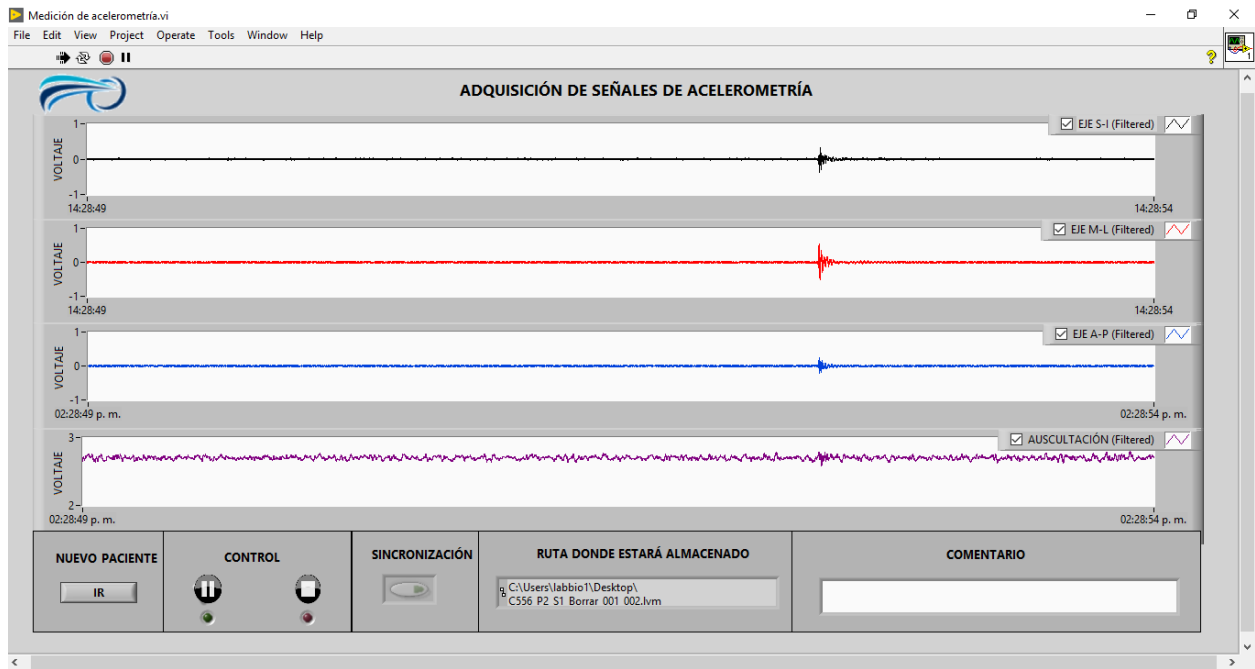


Figure 3-3. MODAC front panel during ACC signal acquisition process

3.2. Pre-processing

The sEMG signal was filtered by a Butterworth-type band pass filter of order 5 with cutoff frequencies between 25-450 Hz. In addition, wavelet denoising was implemented using a db 5-type mother wavelet with 5 decomposition levels, the threshold selection rule was *minimaxi*, the type of thresholding was soft and the multiplicative threshold rescaling mln [99].

The ACC signals were filtered by implementing a bandpass filter type Butterworth between 0.1-3000 Hz. This filter is implemented with a low cutoff frequency in order to eliminate very low-frequency noise and DC components.

The individual analysis of the ACC signals allowed to identify behaviors not related to swallowing. Their elimination was achieved through the manual implementation of wavelet denoising after the identification and segmentation of swallows and non-swallows.

3.2.1. Wavelet denoising

The search for optimal parameters for the filtering of the ACC signals yielded to increase the signal-to-noise ratio. It showed that the use of certain wavelets (db 2 to 6 and Symlet 3

to 5), as well as the implementation of 7, 8, and 9 decomposition levels, reduced the SNR. It was identified that the rule *sqtwolog* for threshold selection and the multiplicative threshold rescaling *sln* did not improve the signal quality. Table **3-1** shows the number of signals that improved their SNR using different combination of parameters with db2.

Table 3-1. Number of signals that increase their SNR. Considering db2 wavelet mother, *heursure* threshold selection rule, *s* type of thresholding. Varying the levels between 7, 8, and 9 and the *mln* and *one* multiplicative threshold rescaling

Signal	Levels	Multiplicative threshold rescaling	Number of signals
AP	7	<i>mln</i>	36
		<i>one</i>	66
	8	<i>mln</i>	33
		<i>one</i>	50
	9	<i>mln</i>	128
		<i>one</i>	78
SI	7	<i>mln</i>	34
		<i>one</i>	52
	8	<i>mln</i>	27
		<i>one</i>	52
	9	<i>mln</i>	150
		<i>one</i>	76
ML	7	<i>mln</i>	31
		<i>one</i>	50
	8	<i>mln</i>	32
		<i>one</i>	53
	9	<i>mln</i>	161
		<i>one</i>	64

The number of signals that showed an increase in SNR was used as a criterion to select the best combination of parameters. The db2 mother wavelet and 9 decomposition levels improved the results, equally, the *heursure* threshold selection rule, *soft* type of thresholding, and the multiplicative threshold rescaling *mln* also contribute positively to the improvement of the quality of the ACC signals. Figure **3-4** shows the scalogram of an identified swallowing segment, as well as filtered and unfiltered noise.

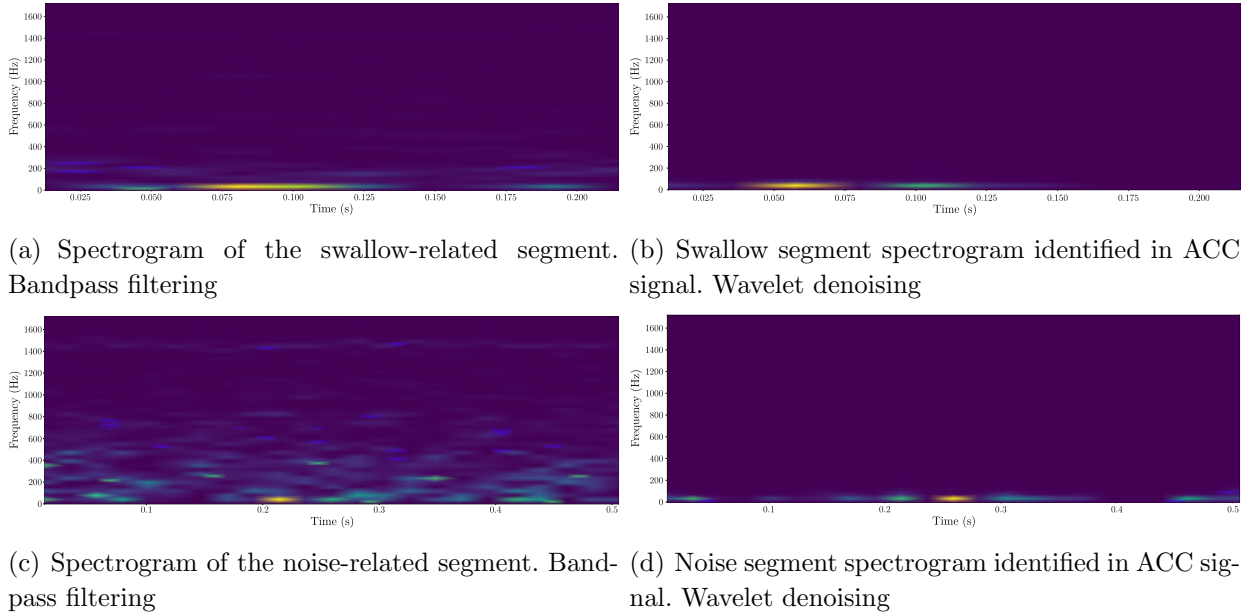


Figure 3-4. ACC spectrograms of swallow and noise, with bandpass filters (a, c), and with optimized wavelet denoising (b, d)

3.3. Feature extraction and feature selection

To obtain the results, feature spaces were created from the full signal, and 1 s, 750 ms, and 500 ms signals considering the application or not application of denoising wavelet. It was also considered the multi-sensor fusion (ACC + sEMG) and the independent information of the signals (ACC and sEMG).

Each feature space obtained from the above considerations was reduced with the three proposed methods (mRMR, PCA, and ROC with thresholds of 0.6, 0.7, and 0.8) in addition to considering each domain calculated as an independent feature space (time, frequency, time-frequency, and information-theoretic features for ACC signals). It is important to note that it was not possible to obtain a ROC 0.8 feature space in all possible scenarios.

All the feature spaces were evaluated by the four described classifiers (SVM, MLP, XG Boost, and KNN). This was done for each of the swallowing tasks. Given the large number of results obtained, this section will analyze the feature spaces that provided the best results, which are presented in Section 3.4

The feature spaces that showed the best results, were analyzed independently, by ACC axis and sEMG channel. Figure 3-5 shows, the percentage of features that belong to each of the analyzed channels, only for sEMG+ACC, because the best results were achieved in this

scenario.

Figure **3-5** shows that at least two ACC channels and all sEMG channels were necessary to discriminate between healthy individuals and dysphagic patients properly. However, in most cases, the presence of ACC features was greater than sEMG features. Analyzing the consistencies independently, and taking into account that different methods of feature selection were chosen for the swallowing tasks, it was found that ACC related features contribute only to 34.21 % of the selected space for 5 mL of yogurt. Otherwise, the AP channel contributes to the 50 % and 63.89 % of the whole feature space for 10 mL of yogurt and 20 mL of water, respectively. The AP channel also contributes with a high percentage in the other consistencies analyzed. Otherwise, the 20 mL of water was the only bolus that allowed the complete elimination of one of the information channels, i.e. the ML channel. However, it was evidenced that this channel was important for other swallowing tasks. It was expected that this channel provides a lower proportion of features, considering that the movement analyzed is not too evident in the swallowing task, in contrast to the AP movement, which is easy to identify during swallowing and, as expected, provides a large amount of information.

Regarding to sEMG channels, it was not possible to identify a clear pattern. For the RIH channel, it was identified that swallowing tasks with volumes of 5 and 20 mL required more features compared to the other sEMG channels. Something similar happens for 10 mL, but with LSH. This is contrary to what would be expected regarding the behavior of these channels since a similar behavior would be expected for all swallowing tasks. However, it should be noted that for the 10 mL swallowing tasks, the RIH channel provided a very reduced amount of information compared to the other volumes.

Accelerometry contributes in most cases with more features regarding the measurements computed in the infrahyoid and suprahyoid muscles by means of sEMG. It is highlighted that the cricoid cartilage favors the protection of the airways, in addition to serving as fixation for the laryngeal muscles, therefore, its function is noteworthy, and may be related to this fact.

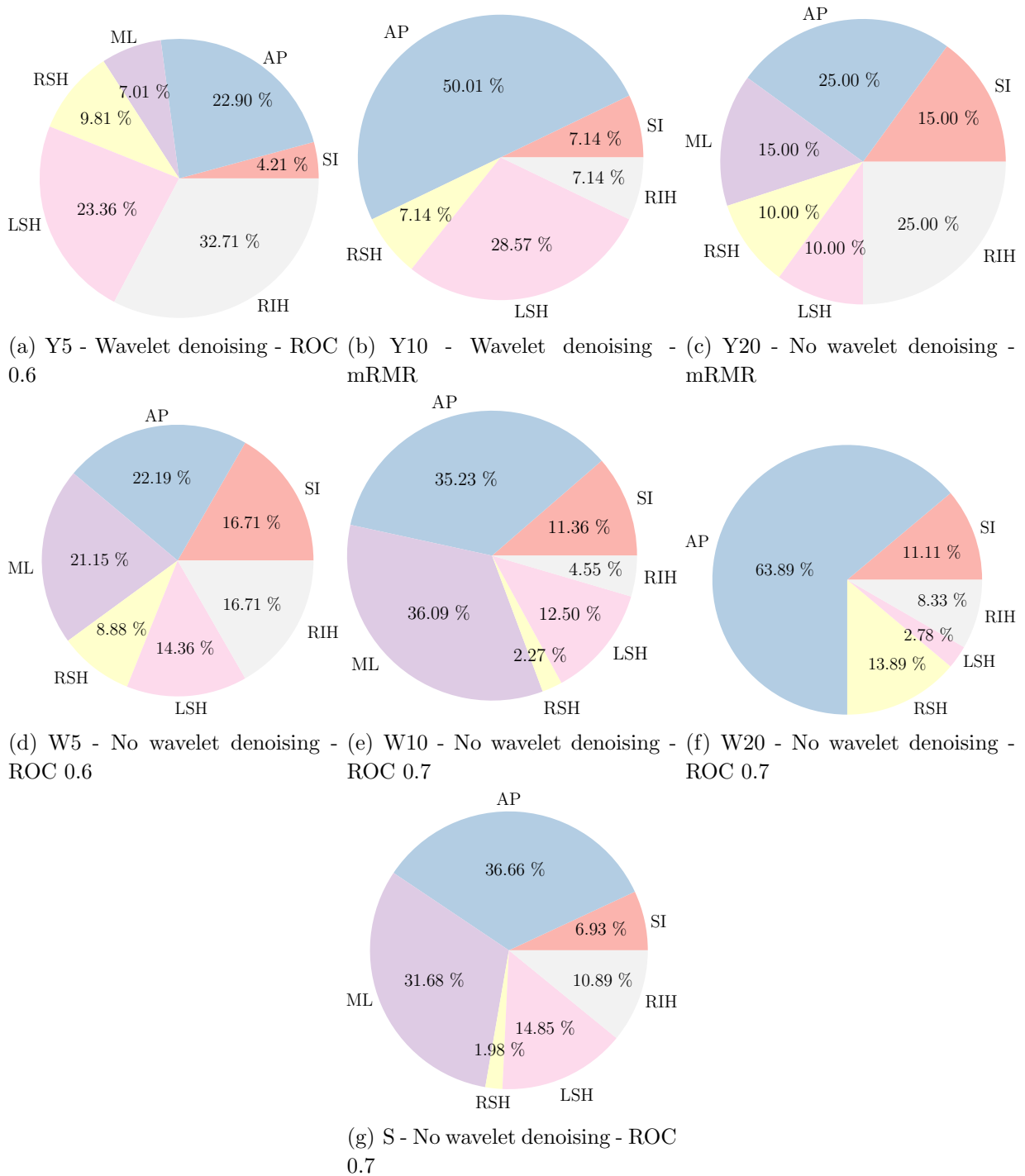


Figure 3-5. Percentage of features per channel analyzed, considering the feature spaces with the highest classification performance.

Table 3-2 shows the number of features selected for each of the swallowing tasks, and the features number per domain. More features are required for characterization of swallowing tasks of 5 ml, compared to the other volumes. This applies also for water in comparison

Table 3-2. Number of features per swallowing task and feature domain

Task	Feature selection	Time	Frequency	Time-Frequency	Non-linear	Total features
Y5	ROC 0.6	102	39	69	4	214
Y10	MRMR	7	1	3	3	14
Y20	MRMR	10	4	5	1	20
S	ROC 0.7	72	9	14	6	101
W5	ROC 0.6	183	59	121	20	383
W10	ROC 0.7	60	9	15	4	88
W20	ROC 0.7	9	7	20	0	36

to yogurt.

The above can also be evidenced in Figure 3-6. It can be seen that the skewness and kurtosis provide lesser information than the mean, standard deviation, maximum and minimum of the analyzed feature. In addition, it is noteworthy that in the two cases where the number of features is small (10 and 20 mL of yogurt) the feature spaces were selected by mRMR, while for the other cases the selected method was the ROC with thresholds of 0.6 and 0.7.

According to the number of features required for the classification of each swallowing task, it can be seen that for low volume more features are required.

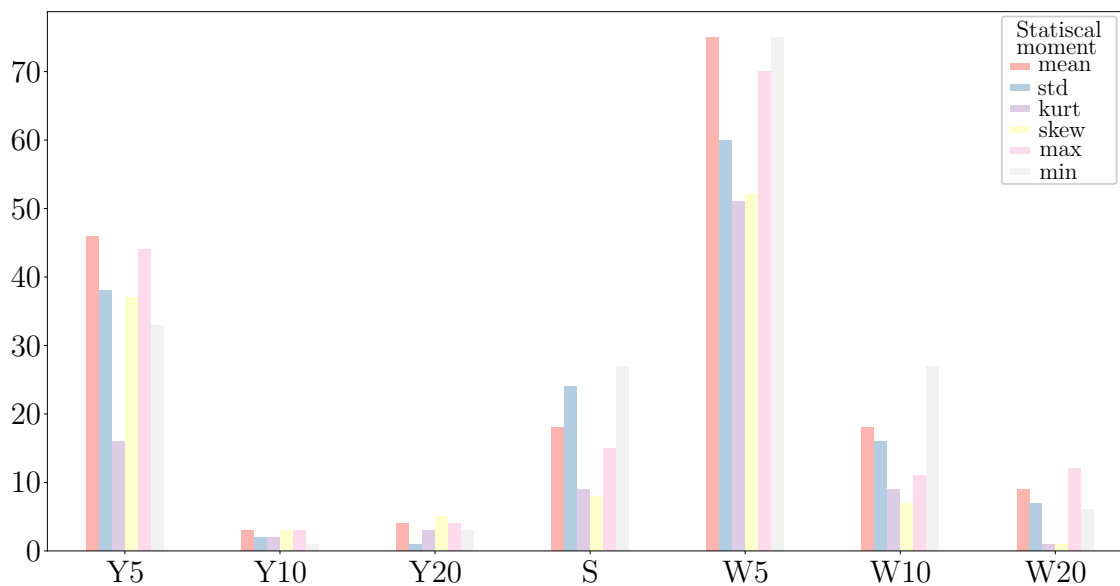


Figure 3-6. Number of features selected per statistical moments, minimum and maximum, according to swallowing task

Likewise, a difference is observed in the number of features necessary to identify healthy or dysphagic subjects from the consistencies evaluated. In the case of water, it was necessary to have a greater number of features than yogurt. It should be considered that for 10 and 20 mL of yogurt, the feature selection method that provided the best AUC was mRMR, and the method eliminates redundant features and contributes to the reduction of dimensionality in a notorious way. A possible explanation for this result may be that swallowing thin liquids in dysphagic population demands additional maneuvers to protect the airway [100, 101]. According to Boiron et al. (1997) there are differences in the duration of swallowing tasks considering density and volume, reporting shorter duration for dense liquids such as yogurt and longer duration for clear liquids such as water, in addition to the difference in duration for the volume of swallowing task [102]. This factor could be related to the need to have a greater number of features for the discrimination of dysphagic subjects.

3.4. Classification

The feature extraction process retrieved 522 ACC features (180 of time, 90 of frequency, 198 of time-frequency, and 54 of non-linear dynamics). In the same way, 396 features of sEMG were calculated (180 of time, 90 of frequency, and 126 of time-frequency). Each of the feature spaces obtained for each of the swallowing tasks was evaluated using different methods for feature selection. In addition, each domain was evaluated separately, as an independent feature space.

The results were evaluated with the AUC, because this work is intended for dysphagia screening, and it seeks for sensitivity-precision trade-off. The best classification results obtained for each swallowing task are presented below. The tasks were evaluated with four classifiers, and three scenarios were considered (ACC, sEMG, and ACC+sEMG), as well as with and without wavelet denoising before the feature extraction.

Although the classifiers were implemented on feature spaces obtained from signal segments, the segmentation process is manual. For this reason, results that can be comparable taking into account the AUC and the sensitivity achieved in the complete signal will be presented. Classification results for each consistency are explained next.

1. Yogurt 5 mL (Y5)

Table **3-3** show that the maximum AUC is 0.90 ± 0.14 with a sensitivity of 0.87 ± 0.17 , using a 750 ms signal without wavelet denoising before feature extraction. For such case, the result was obtained from the implementation of the ROC based feature reduction, with a threshold of 0.6 and an MLP as a classification algorithm.

Furthermore, the use of the full signal, regardless of the use of wavelet denoising, provides comparable results, with AUC of 0.88 ± 0.16 and a sensitivity of 0.87 ± 0.23 for wavelet denoising and AUC of 0.87 ± 0.11 with a sensitivity of 0.87 ± 0.17 without wavelet denoising. In both cases, these results were obtained by implementing a KNN and features selected by the ROC with a threshold of 0.8 and 0.7, respectively. It is important to note that the kNN for this swallowing task retrieves comparable results to the other algorithms, which reduces the computational cost.

Table 3-3. Classification results Y5 (Full signal, 1 s, 750 ms, 500 ms). The best results are highlighted

Signal size	Wavelet denoising	Signal	Classifier	Feature selection	AUC	F1 score	Accuracy	Precision	Sensitivity
Full signal	✓	ACC+sEMG	KNN	ROC 0.6	0.88 ± 0.16	0.87 ± 0.19	0.88 ± 0.16	0.89 ± 0.18	0.87 ± 0.23
		ACC	XGBoost	MRMR	0.82 ± 0.17	0.84 ± 0.14	0.82 ± 0.17	0.81 ± 0.20	0.90 ± 0.16
		sEMG	MLP	ROC 0.8	0.75 ± 0.20	0.70 ± 0.30	0.75 ± 0.20	0.74 ± 0.33	0.70 ± 0.33
	✗	ACC+sEMG	KNN	ROC 0.7	0.87 ± 0.11	0.86 ± 0.11	0.86 ± 0.11	0.88 ± 0.15	0.87 ± 0.17
		ACC	SVM	ROC 0.7	0.80 ± 0.15	0.80 ± 0.14	0.80 ± 0.15	0.80 ± 0.19	0.83 ± 0.18
		sEMG	SVM	ROC 0.6	0.77 ± 0.20	0.76 ± 0.20	0.76 ± 0.20	0.76 ± 0.22	0.80 ± 0.23
1 s	✓	ACC+sEMG	XGBoost	MRMR	0.80 ± 0.13	0.82 ± 0.10	0.80 ± 0.13	0.78 ± 0.17	0.90 ± 0.16
		ACC	KNN	ROC 0.6	0.72 ± 0.14	0.64 ± 0.19	0.73 ± 0.14	0.89 ± 0.18	0.55 ± 0.27
		sEMG	XGBoost	MRMR	0.77 ± 0.12	0.79 ± 0.10	0.76 ± 0.11	0.73 ± 0.15	0.90 ± 0.16
	✗	ACC+sEMG	SVM	ROC 0.6	0.82 ± 0.15	0.83 ± 0.16	0.83 ± 0.15	0.80 ± 0.19	0.88 ± 0.19
		ACC	XGBoost	MRMR	0.75 ± 0.14	0.79 ± 0.12	0.75 ± 0.14	0.69 ± 0.14	0.93 ± 0.14
		sEMG	SVM	ROC 0.6	0.80 ± 0.19	0.80 ± 0.18	0.79 ± 0.20	0.80 ± 0.22	0.83 ± 0.18
750 ms	✓	ACC+sEMG	XGBoost	ROC 0.7	0.78 ± 0.18	0.81 ± 0.16	0.78 ± 0.18	0.73 ± 0.20	0.95 ± 0.16
		ACC	XGBoost	Time-Frequency	0.74 ± 0.18	0.78 ± 0.16	0.74 ± 0.18	0.70 ± 0.21	0.92 ± 0.18
		sEMG	XGBoost	ROC 0.7	0.83 ± 0.22	0.86 ± 0.18	0.83 ± 0.23	0.80 ± 0.23	0.97 ± 0.11
	✗	ACC+sEMG	MLP	ROC 0.6	0.90 ± 0.14	0.89 ± 0.14	0.90 ± 0.14	0.93 ± 0.14	0.87 ± 0.17
		ACC	XGBoost	MRMR	0.68 ± 0.13	0.71 ± 0.12	0.68 ± 0.13	0.64 ± 0.10	0.82 ± 0.20
		sEMG	MLP	ROC 0.6	0.83 ± 0.21	0.83 ± 0.20	0.83 ± 0.21	0.84 ± 0.24	0.87 ± 0.23
500 ms	✓	ACC+sEMG	XGBoost	MRMR	0.73 ± 0.18	0.75 ± 0.15	0.73 ± 0.18	0.76 ± 0.22	0.83 ± 0.24
		ACC	SVM	ROC 0.6	0.72 ± 0.14	0.64 ± 0.28	0.71 ± 0.13	0.68 ± 0.28	0.67 ± 0.35
		sEMG	XGBoost	MRMR	0.73 ± 0.14	0.76 ± 0.12	0.73 ± 0.15	0.72 ± 0.21	0.87 ± 0.17
	✗	ACC+sEMG	KNN	ROC 0.6	0.73 ± 0.12	0.70 ± 0.13	0.73 ± 0.11	0.82 ± 0.19	0.67 ± 0.22
		ACC	MLP	ROC 0.6	0.63 ± 0.26	0.58 ± 0.33	0.64 ± 0.25	0.57 ± 0.33	0.60 ± 0.38
		sEMG	SVM	Time	0.73 ± 0.14	0.64 ± 0.26	0.73 ± 0.14	0.79 ± 0.33	0.60 ± 0.31

2. Yogurt 10 mL (Y10)

Table 3-4 presents the best results obtained for the 10 mL of yogurt task. In this case, a maximum AUC of 0.85 was obtained in two cases. In the first case, the AUC was 0.85 ± 0.15 and a sensitivity of 0.93 ± 0.14 , obtained through the extraction of features applied to the full signal and wavelet denoising. The classification method used to achieve this result was the XGBoost applied on the set of features obtained by applying mRMR. In the second case, a AUC of 0.85 ± 0.17 was obtained with a sensitivity of 0.90 ± 0.16 , however in this case the result was obtained with 1 second of the signal with the implementation wavelet denoising, features reduced by ROC with a threshold of 0.6 and a XGBoost, like the previous case.

Table 3-4. Classification results Y10 (Full signal, 1 s, 750 ms, 500 ms). The best results are highlighted

Signal size	Wavelet denoising	Signal	Classifier	Feature selection	AUC	F1	Accuracy	Precision	Sensitivity
Full signal	✓	ACC+sEMG	XGBoost	MRMR	0.85 ± 0.15	0.85 ± 0.15	0.84 ± 0.17	0.82 ± 0.21	0.93 ± 0.14
		ACC	XGBoost	ROC 0.7	0.80 ± 0.15	0.79 ± 0.17	0.79 ± 0.16	0.78 ± 0.20	0.87 ± 0.23
		sEMG	XGBoost	ROC 0.6	0.70 ± 0.15	0.65 ± 0.27	0.69 ± 0.16	0.66 ± 0.31	0.73 ± 0.34
	✗	ACC+sEMG	MLP	MRMR	0.84 ± 0.17	0.82 ± 0.18	0.84 ± 0.17	0.90 ± 0.22	0.78 ± 0.19
		ACC	SVM	MRMR	0.78 ± 0.19	0.75 ± 0.22	0.79 ± 0.19	0.84 ± 0.22	0.73 ± 0.30
		sEMG	KNN	ROC 0.6	0.77 ± 0.25	0.77 ± 0.26	0.77 ± 0.26	0.73 ± 0.27	0.83 ± 0.27
1 s	✓	ACC+sEMG	XGBoost	ROC 0.7	0.85 ± 0.17	0.86 ± 0.15	0.84 ± 0.18	0.85 ± 0.21	0.90 ± 0.16
		ACC	KNN	ROC 0.6	0.66 ± 0.12	0.60 ± 0.16	0.67 ± 0.12	0.73 ± 0.24	0.55 ± 0.21
		sEMG	KNN	ROC 0.7	0.74 ± 0.14	0.72 ± 0.15	0.74 ± 0.14	0.77 ± 0.22	0.75 ± 0.24
	✗	ACC+sEMG	MLP	ROC 0.6	0.77 ± 0.25	0.75 ± 0.24	0.77 ± 0.25	0.82 ± 0.26	0.77 ± 0.31
		ACC	KNN	ROC 0.6	0.65 ± 0.28	0.59 ± 0.33	0.66 ± 0.27	0.66 ± 0.37	0.60 ± 0.37
		sEMG	KNN	ROC 0.6	0.80 ± 0.17	0.75 ± 0.21	0.80 ± 0.17	0.90 ± 0.21	0.70 ± 0.28
750 ms	✓	ACC+sEMG	XGBoost	MRMR	0.82 ± 0.23	0.77 ± 0.32	0.81 ± 0.23	0.78 ± 0.34	0.83 ± 0.36
		ACC	MLP	ROC 0.6	0.73 ± 0.17	0.64 ± 0.28	0.74 ± 0.16	0.73 ± 0.34	0.60 ± 0.30
		sEMG	SVM	ROC 0.6	0.73 ± 0.20	0.68 ± 0.30	0.73 ± 0.19	0.65 ± 0.31	0.77 ± 0.35
	✗	ACC+sEMG	XGBoost	MRMR	0.83 ± 0.16	0.82 ± 0.18	0.82 ± 0.17	0.79 ± 0.20	0.90 ± 0.22
		ACC	XGBoost	MRMR	0.78 ± 0.16	0.80 ± 0.14	0.77 ± 0.16	0.71 ± 0.18	0.93 ± 0.14
		sEMG	SVM	ROC 0.6	0.81 ± 0.22	0.78 ± 0.26	0.81 ± 0.22	0.78 ± 0.24	0.78 ± 0.29
500 ms	✓	ACC+sEMG	MLP	PCA	0.79 ± 0.15	0.71 ± 0.29	0.80 ± 0.13	0.81 ± 0.32	0.68 ± 0.34
		ACC	XGBoost	MRMR	0.70 ± 0.17	0.71 ± 0.17	0.69 ± 0.17	0.67 ± 0.20	0.80 ± 0.23
		sEMG	KNN	ROC 0.7	0.72 ± 0.17	0.70 ± 0.20	0.71 ± 0.17	0.73 ± 0.24	0.75 ± 0.29
	✗	ACC+sEMG	MLP	ROC 0.6	0.80 ± 0.19	0.73 ± 0.31	0.82 ± 0.17	0.80 ± 0.32	0.70 ± 0.32
		ACC	KNN	MRMR	0.78 ± 0.18	0.76 ± 0.21	0.79 ± 0.18	0.78 ± 0.21	0.77 ± 0.26
		sEMG	KNN	ROC 0.6	0.75 ± 0.28	0.72 ± 0.32	0.76 ± 0.28	0.77 ± 0.35	0.70 ± 0.32

3. Yogurt 20 mL (Y20)

Table 3-5 shows the results obtained with 20 mL of yogurt, where a AUC of 0.92 ± 0.10 and sensitivity of 0.95 ± 0.16 were achieved. Results were obtained without wavelet denoising, and a XGBoost classifier was applied to a reduced feature space by MRMR.

Although an AUC and sensitivity were lower than those presented for this swallowing activity, the implementation of classifiers on 750 ms signals provides a result that can be taken into account. For this case, with the implementation of the wavelet filter prior to the feature extraction, as well as the reduction of the features space through MRMR and XGBoost, they provide an AUC of 0.82 ± 0.18 and a sensitivity of 0.88 ± 0.19 .

Table 3-5. Classification results Y20 (Full signal, 1 s, 750 ms, 500 ms). The best results are highlighted

Signal size	Wavelet denoising	Signal	Classifier	Feature selection	AUC	F1 score	Accuracy	Precision	Sensitivity
Full signal	✓	ACC+sEMG	XGBoost	MRMR	0.84 ± 0.21	0.82 ± 0.23	0.84 ± 0.21	0.85 ± 0.25	0.82 ± 0.24
		ACC	MLP	PCA	0.82 ± 0.16	0.80 ± 0.16	0.81 ± 0.18	0.87 ± 0.22	0.8 ± 0.22
		sEMG	XGBoost	MRMR	0.79 ± 0.16	0.73 ± 0.29	0.79 ± 0.14	0.67 ± 0.28	0.82 ± 0.34
	✗	ACC+sEMG	XGBoost	MRMR	0.92 ± 0.10	0.92 ± 0.12	0.93 ± 0.10	0.92 ± 0.14	0.95 ± 0.16
		ACC	KNN	ROC 0.7	0.86 ± 0.11	0.84 ± 0.13	0.85 ± 0.12	0.89 ± 0.18	0.85 ± 0.20
		sEMG	KNN	ROC 0.7	0.84 ± 0.19	0.84 ± 0.19	0.83 ± 0.19	0.83 ± 0.24	0.88 ± 0.19
1 s	✓	ACC+sEMG	MLP	ROC 0.6	0.81 ± 0.15	0.78 ± 0.18	0.81 ± 0.16	0.87 ± 0.22	0.75 ± 0.23
		ACC	MLP	ROC 0.6	0.71 ± 0.21	0.56 ± 0.41	0.73 ± 0.18	0.57 ± 0.42	0.58 ± 0.44
		sEMG	KNN	ROC 0.7	0.78 ± 0.14	0.71 ± 0.19	0.78 ± 0.14	0.88 ± 0.19	0.65 ± 0.27
	✗	ACC+sEMG	MLP	Time-Frequency	0.77 ± 0.19	0.74 ± 0.20	0.77 ± 0.19	0.82 ± 0.25	0.73 ± 0.25
		ACC	XGBoost	MRMR	0.72 ± 0.20	0.70 ± 0.20	0.70 ± 0.21	0.71 ± 0.28	0.77 ± 0.26
		sEMG	XGBoost	ROC 0.7	0.76 ± 0.16	0.76 ± 0.14	0.75 ± 0.18	0.78 ± 0.24	0.82 ± 0.20
750 ms	✓	ACC+sEMG	XGBoost	MRMR	0.82 ± 0.18	0.82 ± 0.17	0.81 ± 0.20	0.82 ± 0.24	0.88 ± 0.19
		ACC	XGBoost	MRMR	0.68 ± 0.19	0.69 ± 0.19	0.67 ± 0.20	0.67 ± 0.26	0.78 ± 0.24
		sEMG	XGBoost	MRMR	0.78 ± 0.22	0.78 ± 0.19	0.76 ± 0.22	0.74 ± 0.25	0.88 ± 0.19
	✗	ACC+sEMG	XGBoost	Time	0.77 ± 0.19	0.73 ± 0.21	0.77 ± 0.19	0.83 ± 0.24	0.73 ± 0.30
		ACC	KNN	MRMR	0.78 ± 0.19	0.77 ± 0.19	0.77 ± 0.19	0.74 ± 0.21	0.83 ± 0.24
		sEMG	MLP	ROC 0.6	0.70 ± 0.16	0.57 ± 0.34	0.73 ± 0.13	0.65 ± 0.39	0.57 ± 0.38
500 ms	✓	ACC+sEMG	XGBoost	MRMR	0.74 ± 0.22	0.75 ± 0.19	0.72 ± 0.23	0.66 ± 0.23	0.92 ± 0.18
		ACC	XGBoost	MRMR	0.78 ± 0.16	0.8 ± 0.14	0.77 ± 0.17	0.73 ± 0.21	0.93 ± 0.14
		sEMG	MLP	ROC 0.7	0.73 ± 0.18	0.58 ± 0.36	0.75 ± 0.17	0.69 ± 0.4	0.57 ± 0.41
	✗	ACC+sEMG	XGBoost	MRMR	0.79 ± 0.15	0.76 ± 0.18	0.78 ± 0.16	0.78 ± 0.22	0.82 ± 0.25
		ACC	MLP	ROC 0.6	0.78 ± 0.18	0.70 ± 0.30	0.78 ± 0.18	0.74 ± 0.33	0.72 ± 0.34
		sEMG	KNN	ROC 0.8	0.77 ± 0.18	0.64 ± 0.37	0.77 ± 0.18	0.66 ± 0.39	0.67 ± 0.41

4. Dry swallowing (S)

Table 3-6 shows the analyses corresponding to dry swallowing, where a AUC of 0.88 ± 0.14 , and sensitivity of 0.90 ± 0.16 were obtained. This result was achieved by implementing an SVM with a reduced feature space using ROC 0.7 over the complete signals without wavelet denoising. However, the implementation of denoising wavelet contributes in the same way to obtain important results regarding the classification of healthy or dysphagic subjects. The sensitivity, obtained with features selected with ROC 0.7 from the full signal with wavelet denoising, and an MLP as classifier were of 0.97 ± 0.11 and the AUC of 0.87 ± 0.15 .

Table 3-6. Classification results S (Full signal, 1 s, 750 ms, 500 ms). The best results are highlighted

Signal size	Wavelet denoising	Signal	Classifier	Feature selection	AUC	F1 score	Accuracy	Precision	Sensitivity	
Full signal	✓	ACC+sEMG	MLP	ROC 0.7	0.87 ± 0.15	0.89 ± 0.11	0.87 ± 0.15	0.85 ± 0.17	0.97 ± 0.11	
		ACC	SVM	ROC 0.7	0.87 ± 0.11	0.86 ± 0.11	0.87 ± 0.11	0.89 ± 0.14	0.87 ± 0.17	
		sEMG	SVM	NONE	0.73 ± 0.20	0.76 ± 0.15	0.73 ± 0.20	0.77 ± 0.23	0.80 ± 0.17	
	✗	ACC+sEMG	SVM	ROC 0.7	0.88 ± 0.14	0.88 ± 0.14	0.88 ± 0.14	0.88 ± 0.14	0.88 ± 0.15	0.9 ± 0.16
		ACC	SVM	MRMR	0.80 ± 0.15	0.81 ± 0.15	0.80 ± 0.15	0.80 ± 0.17	0.83 ± 0.18	
		sEMG	KNN	ROC 0.6	0.80 ± 0.15	0.78 ± 0.16	0.80 ± 0.15	0.89 ± 0.18	0.73 ± 0.21	
1 s	✓	ACC+sEMG	KNN	ROC 0.6	0.80 ± 0.19	0.78 ± 0.22	0.80 ± 0.19	0.84 ± 0.21	0.77 ± 0.27	
		ACC	KNN	MRMR	0.68 ± 0.18	0.68 ± 0.18	0.68 ± 0.18	0.74 ± 0.24	0.67 ± 0.22	
		sEMG	XGBoost	ROC 0.6	0.77 ± 0.14	0.79 ± 0.12	0.77 ± 0.14	0.79 ± 0.20	0.83 ± 0.18	
	✗	ACC+sEMG	MLP	ROC 0.6	0.77 ± 0.16	0.72 ± 0.28	0.77 ± 0.16	0.74 ± 0.31	0.73 ± 0.31	
		ACC	XGBoost	MRMR	0.68 ± 0.12	0.68 ± 0.16	0.68 ± 0.12	0.67 ± 0.15	0.73 ± 0.26	
		sEMG	KNN	ROC 0.6	0.78 ± 0.16	0.76 ± 0.20	0.78 ± 0.16	0.81 ± 0.18	0.77 ± 0.27	
750 ms	✓	ACC+sEMG	XGBoost	Frequency	0.70 ± 0.15	0.77 ± 0.11	0.70 ± 0.15	0.64 ± 0.11	0.97 ± 0.11	
		ACC	SVM	ROC 0.7	0.68 ± 0.15	0.71 ± 0.15	0.68 ± 0.15	0.66 ± 0.16	0.80 ± 0.23	
		sEMG	KNN	ROC 0.7	0.63 ± 0.11	0.61 ± 0.16	0.63 ± 0.11	0.68 ± 0.19	0.63 ± 0.29	
	✗	ACC+sEMG	MLP	ROC 0.7	0.77 ± 0.18	0.78 ± 0.18	0.77 ± 0.18	0.78 ± 0.21	0.83 ± 0.24	
		ACC	SVM	MRMR	0.72 ± 0.11	0.69 ± 0.15	0.72 ± 0.11	0.78 ± 0.2	0.67 ± 0.22	
		sEMG	SVM	MRMR	0.73 ± 0.20	0.70 ± 0.20	0.73 ± 0.20	0.85 ± 0.21	0.67 ± 0.27	
500 ms	✓	ACC+sEMG	SVM	MRMR	0.83 ± 0.18	0.82 ± 0.20	0.83 ± 0.18	0.83 ± 0.19	0.83 ± 0.24	
		ACC	KNN	ROC 0.7	0.68 ± 0.12	0.67 ± 0.13	0.68 ± 0.12	0.77 ± 0.21	0.67 ± 0.22	
		sEMG	KNN	ROC 0.7	0.72 ± 0.19	0.72 ± 0.19	0.72 ± 0.19	0.73 ± 0.22	0.73 ± 0.21	
	✗	ACC+sEMG	SVM	ROC 0.6	0.75 ± 0.20	0.72 ± 0.24	0.75 ± 0.20	0.74 ± 0.21	0.73 ± 0.31	
		ACC	KNN	ROC 0.6	0.72 ± 0.18	0.68 ± 0.22	0.72 ± 0.18	0.74 ± 0.19	0.67 ± 0.27	
		sEMG	XGBoost	ROC 0.7	0.75 ± 0.12	0.78 ± 0.10	0.75 ± 0.12	0.75 ± 0.18	0.87 ± 0.17	

5. Water 5 mL (W5)

For 5 mL of water (see Table 3-7), it was evidenced that the best case achieved a ROC 0.9 ± 0.09 and a sensitivity of 0.87 ± 0.17 . Obtained over the full signals without the implementation of wavelet denoising, a MLP as a classification method, and selection method ROC 0.6.

Likewise, the classification using 500 ms signals showed that they can a *good* option, considering that it reached an AUC of 0.83 ± 0.16 and a sensitivity of 0.86 ± 0.24 by implementing wavelet denoising on a reduced feature space using ROC 0.6 and an MLP as a classifier.

Table 3-7. Classification results W5 (Full signal, 1 s, 750 ms, 500 ms). The best results are highlighted

Signal size	Wavelet denoising	Signal	Classifier	Feature selection	AUC	F1 score	Accuracy	Precision	Sensitivity
Full signal	✓	ACC+sEMG	SVM	MRMR	0.86 ± 0.16	0.8 ± 0.30	0.86 ± 0.15	0.85 ± 0.32	0.78 ± 0.33
		ACC	XGBoost	ROC 0.8	0.81 ± 0.12	0.81 ± 0.13	0.81 ± 0.12	0.8 ± 0.14	0.85 ± 0.20
		sEMG	XGBoost	ROC 0.7	0.80 ± 0.15	0.82 ± 0.13	0.79 ± 0.16	0.8 ± 0.22	0.90 ± 0.16
	✗	ACC+sEMG	MLP	ROC 0.6	0.90 ± 0.09	0.89 ± 0.10	0.90 ± 0.09	0.95 ± 0.11	0.87 ± 0.17
		ACC	XGBoost	NONE	0.77 ± 0.12	0.79 ± 0.11	0.76 ± 0.11	0.71 ± 0.12	0.90 ± 0.16
		sEMG	KNN	Time	0.87 ± 0.13	0.82 ± 0.19	0.86 ± 0.13	0.97 ± 0.11	0.77 ± 0.27
1 s	✓	ACC+sEMG	MLP	ROC 0.6	0.80 ± 0.15	0.76 ± 0.19	0.79 ± 0.15	0.85 ± 0.20	0.73 ± 0.26
		ACC	MLP	ROC 0.6	0.79 ± 0.16	0.8 ± 0.16	0.79 ± 0.16	0.75 ± 0.19	0.88 ± 0.19
		sEMG	XGBoost	MRMR	0.73 ± 0.14	0.74 ± 0.12	0.73 ± 0.14	0.71 ± 0.16	0.80 ± 0.17
	✗	ACC+sEMG	KNN	ROC 0.7	0.77 ± 0.16	0.76 ± 0.17	0.76 ± 0.17	0.79 ± 0.22	0.77 ± 0.22
		ACC	SVM	ROC 0.6	0.66 ± 0.13	0.51 ± 0.3	0.67 ± 0.12	0.66 ± 0.39	0.45 ± 0.31
		sEMG	KNN	ROC 0.6	0.78 ± 0.11	0.78 ± 0.10	0.78 ± 0.12	0.82 ± 0.20	0.80 ± 0.17
750 ms	✓	ACC+sEMG	KNN	ROC 0.7	0.73 ± 0.2	0.72 ± 0.19	0.73 ± 0.19	0.79 ± 0.24	0.73 ± 0.26
		ACC	XGBoost	ROC 0.6	0.63 ± 0.18	0.64 ± 0.17	0.64 ± 0.18	0.65 ± 0.22	0.67 ± 0.21
		sEMG	KNN	ROC 0.7	0.73 ± 0.20	0.72 ± 0.19	0.73 ± 0.19	0.79 ± 0.24	0.73 ± 0.26
	✗	ACC+sEMG	KNN	ROC 0.6	0.75 ± 0.21	0.67 ± 0.31	0.75 ± 0.21	0.77 ± 0.35	0.63 ± 0.33
		ACC	KNN	ROC 0.7	0.74 ± 0.18	0.73 ± 0.20	0.75 ± 0.18	0.76 ± 0.21	0.78 ± 0.29
		sEMG	KNN	ROC 0.7	0.73 ± 0.18	0.68 ± 0.21	0.73 ± 0.18	0.84 ± 0.24	0.67 ± 0.31
500 ms	✓	ACC+sEMG	MLP	ROC 0.6	0.83 ± 0.16	0.82 ± 0.18	0.83 ± 0.16	0.87 ± 0.17	0.83 ± 0.24
		ACC	KNN	ROC 0.7	0.72 ± 0.19	0.71 ± 0.22	0.71 ± 0.20	0.68 ± 0.20	0.77 ± 0.27
		sEMG	XGBoost	MRMR	0.68 ± 0.2	0.64 ± 0.27	0.68 ± 0.20	0.68 ± 0.33	0.67 ± 0.31
	✗	ACC+sEMG	KNN	MRMR	0.77 ± 0.16	0.73 ± 0.21	0.76 ± 0.16	0.82 ± 0.20	0.73 ± 0.31
		ACC	XGBoost	ROC 0.6	0.65 ± 0.21	0.69 ± 0.22	0.65 ± 0.21	0.60 ± 0.19	0.83 ± 0.28
		sEMG	KNN	AUC 0.6	0.71 ± 0.21	0.67 ± 0.22	0.70 ± 0.21	0.78 ± 0.27	0.65 ± 0.28

6. Water 10 mL (W10)

Table 3-8 shows that the implementation of an SVM on a feature space obtained from the full signal without the wavelet denoising and reduced by the ROC 0.7 method retrieves a AUC of 0.88 ± 0.16 with a sensitivity of 0.87 ± 0.23 .

It is also evident that the results obtained from the analysis of a feature space obtained with ROC 0.7 from the complete signal with the implementation of denoising wavelet can be comparable with an AUC of 0.87 ± 0.17 and a sensitivity of 0.83 ± 0.24 .

Table 3-8. Classification results W10 (Full signal, 1 s, 750 ms, 500 ms). The best results are highlighted

Size signal	Wavelet denoising	Signal	Classifier	Feature selection	AUC	F1 score	Accuracy	Precision	Sensitivity	
Full signal	✓	ACC+sEMG	MLP	ROC 0.7	0.87 ± 0.17	0.85 ± 0.20	0.86 ± 0.18	0.90 ± 0.21	0.83 ± 0.24	
		ACC	SVM	ROC 0.7	0.87 ± 0.11	0.85 ± 0.11	0.86 ± 0.11	0.87 ± 0.17	0.87 ± 0.17	
		sEMG	XGBoost	MRMR	0.71 ± 0.17	0.69 ± 0.19	0.71 ± 0.17	0.72 ± 0.23	0.73 ± 0.25	
	✗	ACC+sEMG	SVM	ROC 0.7	0.88 ± 0.16	0.86 ± 0.19	0.87 ± 0.16	0.88 ± 0.19	0.87 ± 0.23	
		ACC	XGBoost	MRMR	0.83 ± 0.16	0.81 ± 0.18	0.82 ± 0.16	0.79 ± 0.19	0.87 ± 0.23	
		sEMG	KNN	ROC 0.6	0.77 ± 0.27	0.74 ± 0.29	0.77 ± 0.27	0.83 ± 0.28	0.72 ± 0.31	
	1 s	✓	ACC+sEMG	MLP	ROC 0.6	0.74 ± 0.19	0.72 ± 0.21	0.75 ± 0.17	0.76 ± 0.22	0.75 ± 0.29
			ACC	MLP	ROC 0.6	0.62 ± 0.13	0.53 ± 0.29	0.64 ± 0.15	0.58 ± 0.37	0.55 ± 0.34
			sEMG	MLP	MRMR	0.72 ± 0.19	0.6 ± 0.34	0.72 ± 0.18	0.73 ± 0.41	0.57 ± 0.38
✗		ACC+sEMG	KNN	ROC 0.7	0.73 ± 0.16	0.73 ± 0.13	0.74 ± 0.15	0.83 ± 0.23	0.77 ± 0.26	
		ACC	XGBoost	ROC 0.6	0.68 ± 0.19	0.68 ± 0.17	0.66 ± 0.19	0.63 ± 0.19	0.82 ± 0.25	
		sEMG	XGBoost	MRMR	0.76 ± 0.14	0.78 ± 0.10	0.77 ± 0.12	0.76 ± 0.17	0.85 ± 0.20	
750 ms		✓	ACC+sEMG	KNN	ROC 0.6	0.75 ± 0.20	0.67 ± 0.29	0.73 ± 0.20	0.75 ± 0.33	0.70 ± 0.37
			ACC	KNN	MRMR	0.68 ± 0.18	0.53 ± 0.33	0.69 ± 0.16	0.71 ± 0.40	0.5 ± 0.39
			sEMG	XGBoost	MRMR	0.61 ± 0.18	0.63 ± 0.16	0.60 ± 0.17	0.59 ± 0.17	0.72 ± 0.22
	✗	ACC+sEMG	KNN	ROC 0.6	0.78 ± 0.27	0.75 ± 0.33	0.78 ± 0.27	0.79 ± 0.33	0.73 ± 0.34	
		ACC	XGBoost	MRMR	0.72 ± 0.21	0.72 ± 0.22	0.71 ± 0.21	0.71 ± 0.23	0.75 ± 0.24	
		sEMG	XGBoost	MRMR	0.73 ± 0.20	0.7 ± 0.27	0.74 ± 0.16	0.66 ± 0.28	0.77 ± 0.32	
	500 ms	✓	ACC+sEMG	MLP	ROC 0.6	0.78 ± 0.22	0.71 ± 0.31	0.76 ± 0.24	0.81 ± 0.35	0.72 ± 0.35
			ACC	MLP	ROC 0.7	0.68 ± 0.22	0.69 ± 0.18	0.66 ± 0.22	0.68 ± 0.26	0.75 ± 0.18
			sEMG	XGBoost	MRMR	0.68 ± 0.21	0.68 ± 0.17	0.66 ± 0.21	0.7 ± 0.25	0.77 ± 0.27
✗		ACC+sEMG	KNN	Time domain	0.74 ± 0.19	0.69 ± 0.30	0.75 ± 0.17	0.7 ± 0.30	0.73 ± 0.34	
		ACC	XGBoost	ROC 0.7	0.82 ± 0.13	0.83 ± 0.12	0.82 ± 0.12	0.82 ± 0.16	0.88 ± 0.19	
		sEMG	KNN	ROC 0.7	0.72 ± 0.23	0.73 ± 0.18	0.72 ± 0.21	0.73 ± 0.24	0.77 ± 0.21	

7. Water 20 mL (W20)

For the 20 mL of water task (see Table 1), a AUC of 0.91 ± 0.15 and a sensitivity of 0.92 ± 0.18 , were obtained by implementing the ROC 0.6. The used features were obtained through the feature extraction applied on 750 ms signals, with the wavelet denoising and an MLP classifier. However, the analysis of other results is necessary. For this case, it was found that the classification of healthy and diphagic subjects from the full signal reached an AUC of 0.89 ± 0.12 and a sensitivity of 0.78 ± 0.24 with wavelet denoising and an AUC of 0.89 ± 0.22 and a sensitivity of 0.82 ± 0.34 without wavelet denoising.

Table 3-9. Classification results W20 (Full signal, 1 s, 750 ms, 500 ms). The best results are highlighted

Signal size	Wavelet denoising	Signal	Classifier	Feature selection	AUC	F1 score	Accuracy	Precision	Sensitivity
Full signal	✓	ACC+sEMG	KNN	ROC 0.6	0.89 ± 0.12	0.86 ± 0.16	0.90 ± 0.11	1.00 ± 0.00	0.78 ± 0.24
		ACC	KNN	ROC 0.8	0.80 ± 0.17	0.73 ± 0.31	0.82 ± 0.15	0.79 ± 0.33	0.72 ± 0.34
		sEMG	KNN	ROC 0.8	0.73 ± 0.17	0.73 ± 0.16	0.73 ± 0.18	0.77 ± 0.25	0.78 ± 0.24
	✗	ACC+sEMG	KNN	ROC 0.6	0.89 ± 0.22	0.85 ± 0.32	0.90 ± 0.19	0.90 ± 0.32	0.82 ± 0.34
		ACC	MLP	Time-Frequency	0.75 ± 0.17	0.73 ± 0.19	0.76 ± 0.16	0.72 ± 0.21	0.77 ± 0.25
		sEMG	KNN	ROC 0.7	0.78 ± 0.19	0.76 ± 0.21	0.78 ± 0.20	0.78 ± 0.24	0.80 ± 0.27
1 s	✓	ACC+sEMG	XGBoost	ROC 0.7	0.77 ± 0.24	0.73 ± 0.33	0.77 ± 0.23	0.68 ± 0.34	0.82 ± 0.34
		ACC	XGBoost	ROC 0.7	0.69 ± 0.16	0.64 ± 0.27	0.72 ± 0.14	0.65 ± 0.31	0.7 ± 0.35
		sEMG	XGBoost	ROC 0.7	0.82 ± 0.17	0.79 ± 0.20	0.82 ± 0.18	0.85 ± 0.20	0.80 ± 0.27
	✗	ACC+sEMG	MLP	ROC 0.6	0.72 ± 0.3	0.65 ± 0.40	0.72 ± 0.29	0.68 ± 0.43	0.63 ± 0.39
		ACC	XGBoost	MRMR	0.71 ± 0.18	0.72 ± 0.18	0.70 ± 0.19	0.63 ± 0.19	0.87 ± 0.22
		sEMG	XGBoost	Time-Frequency	0.72 ± 0.12	0.70 ± 0.13	0.70 ± 0.14	0.68 ± 0.20	0.83 ± 0.27
750 ms	✓	ACC+sEMG	MLP	ROC 0.7	0.91 ± 0.15	0.92 ± 0.14	0.92 ± 0.14	0.94 ± 0.12	0.92 ± 0.18
		ACC	SVM	ROC 0.7	0.79 ± 0.16	0.79 ± 0.13	0.79 ± 0.15	0.82 ± 0.20	0.83 ± 0.22
		sEMG	XGBoost	MRMR	0.76 ± 0.15	0.73 ± 0.16	0.76 ± 0.16	0.8 ± 0.22	0.75 ± 0.27
	✗	ACC+sEMG	SVM	ROC 0.6	0.78 ± 0.17	0.66 ± 0.37	0.78 ± 0.18	0.68 ± 0.39	0.7 ± 0.42
		ACC	KNN	ROC 0.7	0.75 ± 0.18	0.69 ± 0.30	0.76 ± 0.16	0.67 ± 0.30	0.73 ± 0.34
		sEMG	KNN	ROC 0.7	0.70 ± 0.19	0.61 ± 0.28	0.71 ± 0.18	0.68 ± 0.33	0.60 ± 0.33
500 ms	✓	ACC+sEMG	KNN	ROC 0.7	0.82 ± 0.15	0.77 ± 0.29	0.84 ± 0.13	0.78 ± 0.31	0.82 ± 0.34
		ACC	XGBoost	ROC 0.7	0.74 ± 0.17	0.75 ± 0.18	0.76 ± 0.16	0.72 ± 0.21	0.85 ± 0.24
		sEMG	XGBoost	MRMR	0.86 ± 0.19	0.83 ± 0.24	0.86 ± 0.19	0.87 ± 0.22	0.83 ± 0.27
	✗	ACC+sEMG	MLP	ROC 0.6	0.83 ± 0.12	0.81 ± 0.17	0.84 ± 0.13	0.87 ± 0.16	0.83 ± 0.27
		ACC	MLP	ROC 0.6	0.79 ± 0.16	0.77 ± 0.2	0.82 ± 0.15	0.85 ± 0.21	0.75 ± 0.26
		sEMG	SVM	ROC 0.7	0.82 ± 0.17	0.75 ± 0.3	0.82 ± 0.15	0.68 ± 0.3	0.85 ± 0.34

It is important to note that in all swallowing tasks, classifiers were analyzed for the ACC and sEMG signals independently and together. However, the best results were given by the fusion of signals. If each of the possible cases is analyzed, considering the length of the signals and the application of wavelet denoising, in a few cases the analysis of ACC or sEMG independently provides the best result.

Figure 3-7 summarizes the previous results according to the AUC achieved for each swallowing task. Although it only shows the achieved AUC, in some cases, the sensitivity was necessary to figure out which of the methods was the best.

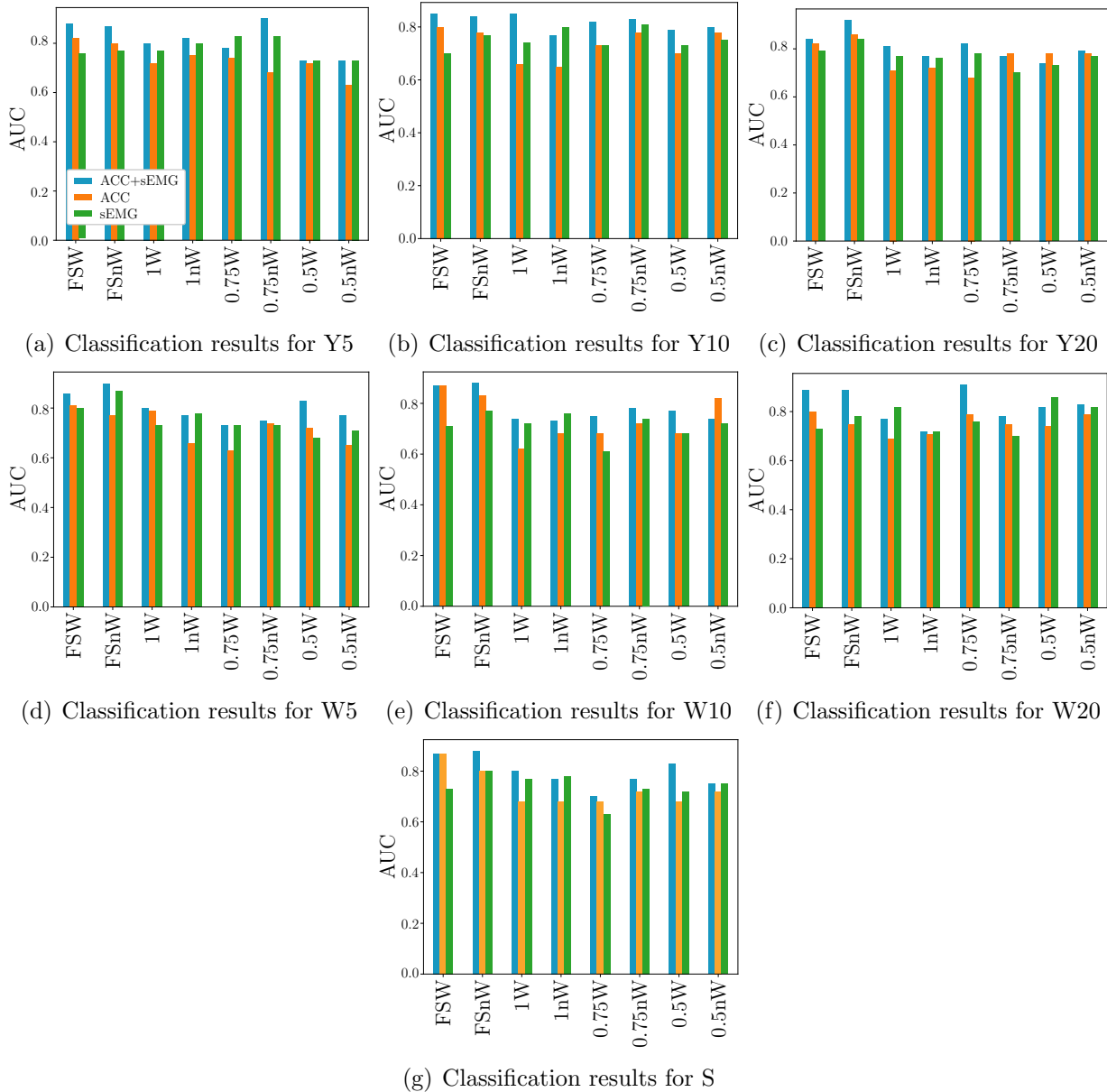


Figure 3-7. Graphic representation of the highest AUC highest. Where: FSW is Full signal with wavelet denoising, FSnW is Full signal without wavelet denoising, 1W is 1 s of signal with wavelet denoising, 1nW is 1 s of signal without wavelet denoising, 0.75W is 750 ms of signal with wavelet denoising, 0.75nW is 750 ms of signal without wavelet denoising, 0.5W is 500 ms of signal with wavelet denoising, 0.5nW is 500 ms of signal without wavelet denoising

From the results obtained, it stands out that for 20 mL of water and 5 mL of yogurt, the highest AUC was obtained using 750 ms signal segments. Some authors have reported differences in the swallowing process of men and women in terms of its duration, with men taking the longest to swallow. Furthermore, these differences can also be seen with respect to anthropological and demographic variables [103]. However, Matthew et al. (1999) estimated that the duration of swallowing apnea is 0.75 ± 0.14 seconds, an event that is directly related to the movement of the cricoid cartilage since it moves to favor the protection of the respiratory tract [103, 104]. It should also be noted that, although several authors report that swallowing lasts approximately 2.5 s, this is for the three stages that compose it, while this research analyzes the oral and pharyngeal stages.

The results obtained from the feature extraction of the ACC and sEMG signals of segments of the original signal are important. Previous research found that calculating descriptors in percentages of the original data produced identical results. In the case of the time domain, it was determined that with 20 % of the data and for the frequency, that with a third of them the results represented the behavior of the complete signal in swallowing [55]. It is also important to consider that using time windows focused on swallowing would eliminate unnecessary information and, using a sliding window, the calculation of descriptors on the changes in the signal at the time of swallowing is given.

Likewise, it can be seen that for 20 mL of water and yogurt the highest AUC is reached compared to the others swallowing. It could be related to the findings of Maria das Graças et al. (2012). They showed that 20 mL of water commonly produces piecemeal deglutition in patients with dysphagia. This observation was consistent in more than 80 % of patients. Thus, this amount of water was called as dysphagia limit, i.e. the limit of liquid that demands partitioning of boluses only in the dysphagic population [105].

Swallowing is a complex process, where different dimensions are related that allow facilitating its understanding, however, most studies, based on biosignals, do so considering a single dimension. Two of the most important dimensions in swallowing are related to the kinematics, which is analyzed through cervical auscultation or accelerometers located in the cricoid cartilage, and the electrophysiological dimension, which is analyzed by mechanomyography, surface electromyography, or needle electromyography.

This work implemented conventional classification algorithms from features extracted by means of overlapping sliding windows on ACC and sEMG signals. Which allowed, from the point of view of signal analysis, the improvement of the quality of the information collected and the reduction of bias and uncertainty [106]. Likewise, the implementation of multiple sensors for the analysis of the same swallowing process allows an understanding of the information considering the two previous dimensions. The existing studies where multimodal

techniques are used are not comparable with our results, considering that they use different sources of information than those used here, complete registers are not compared, the population used is usually healthy or dysphagic, normal swallows are compared with abnormal swallows, or manual segmentation of signals is implemented, a process that was not applied in this study.

However, a research implemented an SVM with information from sEMG and bioimpedance signals to detect swallows in healthy and dysphagic people. A sensitivity of 96.1 % and a precision of 96.6 % were obtained in healthy individuals. Likewise, the results showed a decrease in the metrics, obtaining 84.1 % and 84.5 %, respectively, in the dysphagic population [75]. It should be considered that this study used a methodology based on two sources of information, however, the main objective is not related to the identification of healthy and dysphagic subjects but to the detection of swallows. Nevertheless, the results obtained in this work, which sought the identification of healthy and dysphagic subjects through swallowing tasks, were shown to be superior in most cases.

Secondly, many accelerometry researchers implement microphones to perform cervical auscultation. However, these studies use a healthy or dysphagic population, but not both groups, and their main objective is usually the detection of normal or abnormal swallowing [107, 108]. For example, Mohammadi et al. used an SVM and neural networks to detect different actions through ACC, achieving an accuracy of $99.26 \pm 0.12\%$ to discriminate voluntary cough and accelerometry signals at rest and an accuracy of $90.20 \pm 3.60\%$ and $80.30 \pm 10.50\%$ when classifying cough and induced cough from other artifacts. From this research it stands out that some results presented could be considered outstanding, however, it is important to note that these were obtained from a single population group and different activities that could be related to swallowing were compared. For example, coughing often occurs in patients with aspiration or penetration. The foregoing means that these results cannot be comparable, but they do mark a starting point in the integration of signals in swallowing.

3.5. Model selection

According to the previous results, there is not a classification model that clearly overcomes the other in terms of performance. So, the three models with their corresponding optimized hyperparameters were used for tests purposes. Such test was performed with 22 individuals exposed in the Section 2.6.3, who did not were included in the training stage.

Tables **3-10**, **3-11** and **3-12** show the mode of the combination of hyperparameters for each model and swallowing task, as well as the parameters implemented for the feature extraction for the test subjects.

Table 3-10. Parameters for feature extraction and MLP hyperparameters

Task	Activation	Alpha	Hidden layer sizes	Solver	Signal size	Wavelet denoising
Y5	tanh	1	10	SGD	750 ms	✗
W5	ReLU	0,0001	10	adam	Full signal	✗
W20	ReLU	0,0001	20	adam	750 ms	✓

Table 3-11. Parameters for feature extraction and XGBoost hyperparameters

Task	Max depth	Weights balancing	Signal size	Wavelet denoising
Y10	5	1	Full signal	✓
Y20	2	10	Full signal	✓

Table 3-12. Parameters for feature extraction and SVM hyperparameters

Task	C	γ	Kernel	Signal size	Wavelet denoising
S	10	0,001	rbf	Full signal	✗
W10	1	0,01	rbf	Full signal	✗

According to the selected models, the MLP was the best classification model for three of the swallowing tasks. On the other hand, SVM and XGBoost, provided each, a good result in two cases. Although KNN, did not achieve the highest performance in any of the swallowing tasks, it provides good results for some cases. It should not be completely excluded from future research.

Table **3-13** shows the behavior of the algorithms for each test subject. Some subjects were classified correctly in all their swallowing tasks. It is important to clarify that the test subjects were chosen without considering the sex, age, or underlying pathology of the patients. Although this can reduce the performance of the algorithms, it also provides more generalized results.

Table 3-13. Classification of test subjects

Group	ID	Y5	Y10	Y20	S	W5	W10	W20
Controls	1	✗	✓	✗	✓	✗	✓	✗
	2	✓	✗	✓	✗	✓	✓	✗
	3	✓	✓	✓	✓	✓	✓	✓
	4	✗	✓	✗	✗	✗	✗	✗
	5	✓	✗	✓	✓	✓	✓	✓
	6	✓	✓	✓	✓	✓	✓	✗
	7	✗	✗	✗	✓	✓	✓	✗
	8	✓	✓	✓	✓	✓	✓	✓
	9	✗	✓	✓	✗	✓	✗	✗
	10	✓	✓	✓	✓	✓	✓	✓
	11	✓	✓	✓	✓	✓	✓	✓
Patients	1	✗	✓	✓	✓	✗	✓	✗
	2	✓	✓	✓	✓	✓	✗	–
	3	✓	✓	✓	✓	✓	✓	✗
	4	✓	✓	✓	✓	✓	✓	✓
	5	✗	✓	–	✓	✓	✓	–
	6	✓	✗	✓	✓	✓	✓	✓
	7	✗	✓	✓	✓	✓	✓	✓
	8	✗	✗	✗	✗	✗	✗	✓
	9	✓	✓	✓	✓	✓	✓	✗
	10	✓	✗	✓	✗	✗	✗	✓
	11	✓	✓	–	✓	–	–	–

Table 3-14 and Figure 3-8 summarize the performance measures obtained in the test database. Accordingly, the 20 mL of water task demands the highest difficulties for discrimination between healthy and dysphagic states.

The swallowing tasks corresponding to 20 mL of yogurt and saliva provided the best classification results for the test subjects, achieving an AUC of 0.81 and a sensitivity of 0.89 for 20 mL of yogurt and 0.77 and 0.82 for the saliva. These tasks were usually completed in most patients, even in patients with severe dysphagia or with feeding tubes where dry swallows are performed. This is important to keep in mind for future developments and for clinical applications.

Table 3-14. Performance measures with the test database. Highlighted results are where the algorithm reached a value greater than 0.8.

Task	AUC	F1 score	Accuracy	Precision	Sensitivity
Y5	0.64	0.64	0.64	0.64	0.64
Y10	0.73	0.73	0.73	0.73	0.73
Y20	0.81	0.80	0.80	0.73	0.89
S	0.77	0.78	0.77	0.75	0.82
W5	0.76	0.74	0.76	0.78	0.70
W10	0.76	0.74	0.76	0.78	0.70
W20	0.54	0.53	0.53	0.45	0.62

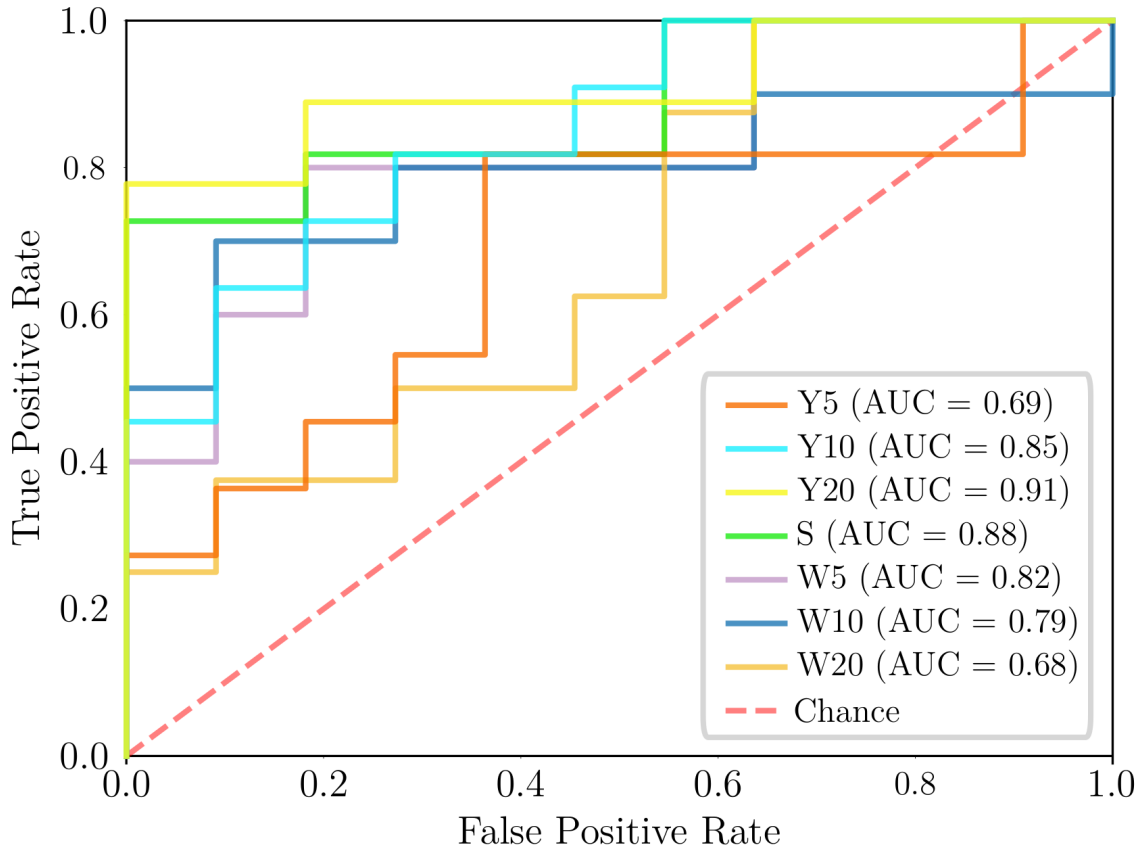


Figure 3-8. ROC curve of each swallowing task for test subjects

Defining a single methodology for the identification of healthy or dysphasic subjects is a complex process that requires further analysis. However, it is evident that the proposed methodology is correct in relation to obtaining swallowing information through different sources (ACC and sEMG) and the feature extraction from such signals. It is important to consider that the features sets used for each of the swallowing activities differ among them,

both in number and in the features selected.

According to the results obtained, the performance of specific swallowing tasks provides valuable information for the identification of dysphagic subjects, these tasks are especially related to the limit volumes of dysphagia (20 mL) and therefore it is advisable to evaluate these swallowing tasks, seeking that patients do not undergo long protocols and present fatigue.

The general methodology could be based on three stages: 1) Recording of ACC and sEMG signals in predefined swallowing tasks (20 mL of water and yogurt especially). 2) Feature extraction by implementing overlapping sliding windows (time and frequency domain and information-theoretic features). 3) Evaluation of the subject's information from the models defined for each of the swallowing tasks.

4. Conclusions and contributions

4.1. Conclusions

This research evaluated sEMG and ACC signals, in healthy and dysphagic subjects. The results made it possible to determine that multi-sensor fusion contributes positively to the improvement of the classification, compared with the classification results using the signals individually. It was observed that in all swallowing tasks the highest AUC reached exceeds 0.85, achieving an AUC higher than 0.9 for the swallowing tasks of 5 and 20 mL of yogurt and water. The results obtained in this study equal and even exceed the results of studies that have implemented multimodal techniques based on cervical auscultation and ACC or sEMG and bioimpedance, as well as studies where these two dimensions are analyzed individually. However, it should be noted that these results are not completely comparable, since they use different bio-signals.

The use of the feature spaces formed by each of the domains, the total of the features, or the one obtained by the application of principal component analysis with semantics are not recommended for the identification of subjects with dysphagia. However, the feature selection methods showed two possible cases that should be considered and that are important to highlight. The implementation of feature selection through Receiver Operating Characteristic using thresholds at 0.6 and 0.7 is an appropriate technique to implement in swallowing tasks where a high number of features are required for classification, such as 5 mL of yogurt, 5, 10 and 20 mL of water and saliva. In the case of 10 and 20 mL of water, the number of required features was much less and could be obtained through the implementation of Minimum Redundancy - Maximum Relevance. The clear liquid (water) showed that the number of necessary features for classification was much higher than in thick liquids (yogurt). It was also evidenced that the mean, the standard deviation, the maximum and minimum, contributed with more features than the skewness and kurtosis.

The feature extraction in signals of 750 ms contributed positively to the classification performance in some swallowing tasks (5 mL of yogurt, and 20 mL of water). In addition, for the cases where signals of 1 s 750 ms, and 500 ms were analyzed, most of the results exceeded an AUC of 0.7, comparable with the results reported as best. Thus, this is a valid methodology to implement for the development of classification algorithms. Furthermore, it can be considered that the swallowing act falls within this time window, and the adjacent

segments do not provide relevant information.

The results obtained in function of AUC showed certain stability between the different applied models, which shows more dependence on the feature spaces than on the applied classification models. Furthermore, this allows, to reduce the overfitting of the models.

One test was applied on 22 subjects, using the best feature spaces and selected classification models, this test showed that the implemented methodology is an option to consider for the development of screening techniques for people with dysphagia, in addition to being economical and non-invasive.

The use of the statistical moments, as well as the minimum and the maximum in the process of feature extraction allowed to show that, although all these descriptors provide important information for the identification of healthy and dysphagic subjects, the mean, variance, minimum, and maximum are recommended.

In another way, the MODAC is an important instrumental contribution developed for the acquisition of ACC signals and their synchronization with the sEMG signals in the swallowing tasks.

From this work, it stands out that, according to our knowledge, it is one of the first works where the electrophysiological and kinematic dimension in swallowing tasks are analyzed, in addition to using a database with a healthy and dysphagic population. Being the main contribution of this work, the contribution to the construction of the state of the art in dysphagia and the multimodal analysis of it

4.2. Limitations and future works

The segmentation of signals from the kinematic events detected using the accelerometer located in the cricoid cartilage was carried out using visual inspection, which introduces errors in said process. Therefore, it is considered important to generate automatic segmentation algorithms validated using instrumental tests such as the VFFS that would allow obtaining direct information on the swallowing process and correlating it with our source information., seeking to improve the results obtained.

The main limitation of this work is the size of the database and the heterogeneous etiologies of dysphasic subjects. Therefore, it is considered important to evaluate the proposed methodology in a broader database that preserves the match by age and sex.

A. Appendix: MODAC block diagram

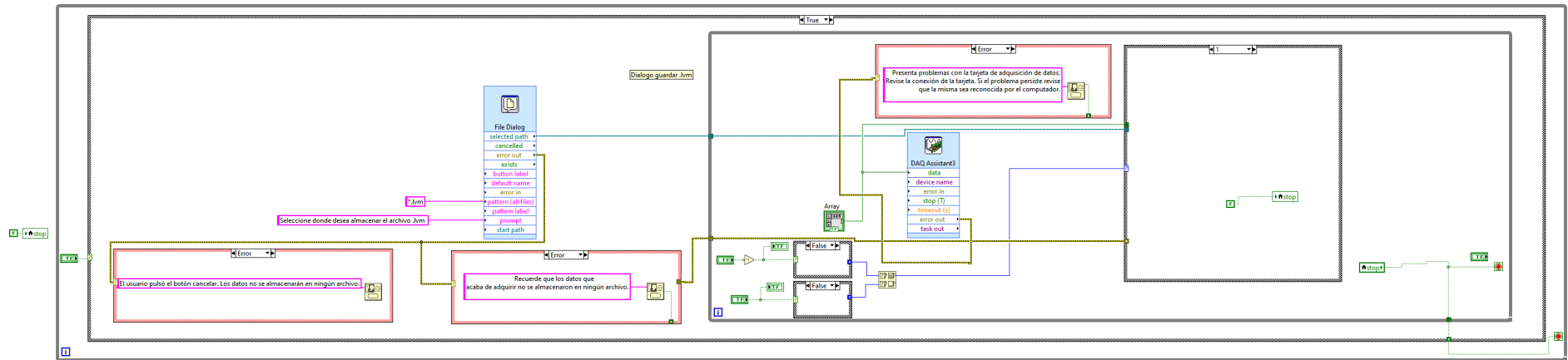


Figure A-1. MODAC block diagram for acquiring EMG synchronized ACC signals

References

- [1] Drozd, D., Mancopes, R., Silva, A., Reppold, C.: Analysis of the Level of Dysphagia, Anxiety, and Nutritional Status Before and After Speech Therapy in Patients with Stroke. *International Archives of Otorhinolaryngology* **18** (2014) 172–177
- [2] Chen, D.F.: Dysphagia in the Hospitalized Patient. *Hospital Medicine Clinics* **6** (2017) 38–52
- [3] Carter, S., Gutierrez, G.: The concurrent validity of three computerized methods of muscle activity onset detection. *Journal of Electromyography and Kinesiology* **25** (2015) 731–741
- [4] Streppel, M., Veder, L.L., Pullens, B., Joosten, K.F.: Swallowing problems in children with a tracheostomy tube. *International Journal of Pediatric Otorhinolaryngology* **124** (2019) 30–33
- [5] Miller, A.J.: The neurobiology of swallowing and dysphagia. *Developmental Disabilities Research Reviews* **14** (2008) 77–86
- [6] Dodds, W.J., Stewart, E.T., Logemann, J.A.: Physiology Pharyngeal and Radiology of the Normal Phases of Swallowing. *AJR. American journal of roentgenology* (1990) 953–963
- [7] Shapira-Galitz, Y., Drendel, M., Yousovich-Ulriech, R., Shtreiffler-Moskovich, L., Wolf, M., Lahav, Y.: Translation and Validation of the Dysphagia Handicap Index in Hebrew-Speaking Patients. *Dysphagia* **34** (2019) 63–72
- [8] Suárez Escudero, J.C., Rueda Vallejo, Z.V., Orozco, A.F.: Disfagia y neurología: ¿una unión indefectible? *Acta Neurológica Colombiana* **34** (2018) 92–100
- [9] Ekberg, O., Hamdy, S., Woisard, V., Wuttge-Hannig, A., Ortega, P.: Social and psychological burden of dysphagia: Its impact on diagnosis and treatment. *Dysphagia* **17** (2002) 139–146
- [10] Hemsley, B., Balandin, S., Sheppard, J.J., Georgiou, A., Hill, S.: A call for dysphagia-related safety incident research in people with developmental disabilities. *Journal of Intellectual and Developmental Disability* **40** (2015) 99–103

-
- [11] Carucci, L.R., Ann Turner, M.: Dysphagia revisited: Common and unusual causes. *Radiographics* **35** (2015) 105–122
- [12] Wilkins, T., Gillies, R.A., Thomas, A.M., Wagner, P.J.: The prevalence of dysphagia in primary care patients: A HimesNet research network study. *Journal of the American Board of Family Medicine* **20** (2007) 144–150
- [13] Ding, X., Gao, J., Xie, C., Xiong, B., Wu, S., Cen, Z., Lou, Y., Lou, D., Xie, F., Luo, W.: Prevalence and clinical correlation of dysphagia in parkinson disease: a study on chinese patients. *European journal of clinical nutrition* **72** (2018) 82–86
- [14] Chadwick, D.D., Jolliffe, J.: A descriptive investigation of dysphagia in adults with intellectual disabilities. *Journal of Intellectual Disability Research* **53** (2009) 29–43
- [15] Smithard, D., O’neill, P., Park, C., Morris, J., Wyatt, R., England, R., Martin, D.: Complications and outcome after acute stroke: does dysphagia matter? *Stroke* **27** (1996) 1200–1204
- [16] Gevers, A.M., Macken, E., Hiele, M., Rutgeerts, P.: A comparison of laser therapy, plastic stents, and expandable metal stents for palliation of malignant dysphagia in patients without a fistula. *Gastrointestinal endoscopy* **48** (1998) 383–388
- [17] Nacci, A., Ursino, F., La Vela, R., Matteucci, F., Mallardi, V., Fattori, B.: Fiberoptic endoscopic evaluation of swallowing (fees): proposal for informed consent. *Acta Otorhinolaryngologica Italica* **28** (2008) 206
- [18] Zammit-Maempel, I., Chapple, C.L., Leslie, P.: Radiation dose in videofluoroscopic swallow studies. *Dysphagia* **22** (2007) 13–15
- [19] Wilson, R.D., Howe, E.C.: A Cost-Effectiveness Analysis of Screening Methods for Dysphagia After Stroke. *PM and R* **4** (2012) 273–282
- [20] Broussard, D.L., Altschuler, S.M.: Central integration of swallow and airway- protective reflexes. *American Journal of Medicine* **108** (2000) 62–67
- [21] Cassiani, R.A., Santos, C.M., Parreira, L.C., Dantas, R.O.: The relationship between the oral and pharyngeal phases of swallowing. *Clinics* **66** (2011) 1385–1388
- [22] Ertekin, C.: Physiological and pathological aspects of oropharyngeal swallowing. *Movement Disorders* **17** (2002) 86–89
- [23] Lang, I.M.: Brain stem control of the phases of swallowing. *Dysphagia* **24** (2009) 333–348

- [24] Pedersen, A., Bardow, A., Jensen, S.B., Nauntofte, B.: Saliva and gastrointestinal functions of taste, mastication, swallowing and digestion. *Oral Diseases* **8** (2002) 117–129
- [25] Silva, A.C.V., Fabio, S.R.C., Dantas, R.O.: A Scintigraphic Study of Oral, Pharyngeal, and Esophageal Transit in Patients with Stroke. *Dysphagia* **23** (2008) 165–171
- [26] Movahedi, F., Kurosu, A., Coyle, J.L., Perera, S., Sejdić, E.: Anatomical directional dissimilarities in tri-axial swallowing accelerometry signals. *IEEE Transactions on Neural Systems and Rehabilitation Engineering* **25** (2017) 447–458
- [27] Tawadros, P.B., Cordato, D., Cathers, I., Burne, J.A.: An electromyographic study of parkinsonian swallowing and its response to levodopa. *Movement Disorders* **27** (2012) 1811–1815
- [28] Suryanarayanan, S., Reddy, N.P., Canilang, E.P.: A fuzzy logic diagnosis system for classification of pharyngeal dysphagia. *International Journal of Bio-Medical Computing* **38** (1995) 207–215
- [29] Hadde, E.K., Nicholson, T.M., Cichero, J.A.: Evaluation of Thickened Fluids Used in Dysphagia Management Using Extensional Rheology. *Dysphagia* **35** (2020) 242–252
- [30] Smith, K.E., Saad, A.R., Hanna, J.P., Tran, T., Jacobs, J., Richter, J.E., Velanovich, V.: Revisional Surgery in Patients with Recurrent Dysphagia after Heller Myotomy. *Journal of Gastrointestinal Surgery* **24** (2020) 991–999
- [31] Potulska, A., Friedman, A., Królicki, L., Spychala, A.: Swallowing disorders in Parkinson’s disease. *Parkinsonism and Related Disorders* **9** (2003) 349–353
- [32] Trapl, M., Enderle, P., Nowotny, M., Teuschl, Y., Matz, K., Dachenhausen, A., Brainin, M.: Dysphagia bedside screening for acute-stroke patients: The gugging swallowing screen. *Stroke* **38** (2007) 2948–2952
- [33] Fernández-Carmona, A., Peñas-Maldonado, L., Yuste-Osorio, E., Díaz-Redondo, A.: Exploración y abordaje de disfagia secundaria a vía aérea artificial. *Medicina Intensiva* **36** (2012) 423–433
- [34] Demir, N., Serel Arslan, S., Ä°nal, Ö., Karaduman, A.A.: Reliability and Validity of the Turkish Eating Assessment Tool (T-EAT-10). *Dysphagia* **31** (2016) 644–649
- [35] Langmore, S.E., Kenneth, S.M., Olsen, N.: Fiberoptic endoscopic examination of swallowing safety: A new procedure. *Dysphagia* **2** (1988) 216–219

-
- [36] Vigotsky, A.D., Halperin, I., Lehman, G.J., Trajano, G.S., Vieira, T.M.: Interpreting signal amplitudes in surface electromyography studies in sport and rehabilitation sciences. *Frontiers in Physiology* **8** (2018)
- [37] Hess, U., Arslan, R., Mauersberger, H., Blaison, C., Dufner, M., Denissen, J.J., Ziegler, M.: Reliability of surface facial electromyography. *Psychophysiology* **54** (2017) 12–23
- [38] Roldan-Vasco, S., Perez-Giraldo, E., Orozco-Duque, A.: Continuous Wavelet Transform for Muscle Activity Detection in Surface EMG Signals During Swallowing. Volume 916 of *Communications in Computer and Information Science*. Springer International Publishing (2018)
- [39] Vaiman, M.: Standardization of surface electromyography utilized to evaluate patients with dysphagia. *Head and Face Medicine* **3** (2007) 1–7
- [40] Cadavid-Arboleda, S., Ramirez-Arbelaez, L., Perez-Giraldo, E., Restrepo-Agudelo, S., Roldan-Vasco, S., Suarez-Escudeto, J.C., G, C.M., Bedoya-Londoño, C., Martinez-Moreno, L., Orozco-Duque, A.: Assessment of Surface Electromyography During Orofacial Praxis in Healthy Subjects. *IFMBE Proceedings* **60** (2017) 520–523
- [41] Roldan-Vasco, S., Restrepo-Agudelo, S., Valencia-Martinez, Y., Orozco-Duque, A.: Automatic detection of oral and pharyngeal phases in swallowing using classification algorithms and multichannel EMG. *Journal of Electromyography and Kinesiology* **43** (2018) 193–200
- [42] Begnoni, G., Cadenas de Llano-Pérula, M., Willems, G., Pellegrini, G., Musto, F., Dellavia, C.: Electromyographic analysis of the oral phase of swallowing in subjects with and without atypical swallowing: A case-control study. *Journal of Oral Rehabilitation* **46** (2019) 927–935
- [43] Perlman, A.L., D, P.: Electromyography in oral and pharyngeal motor disorders. *GI Motility online* (2006) 1–31
- [44] Haggstrom, M.: Medical gallery of mikael haggstrom 2014. *WikiJournal of Medicine* **1** (2014) 1–53
- [45] Ashiga, H., Takei, E., Magara, J., Takeishi, R., Tsujimura, T., Nagoya, K., Inoue, M.: Effect of attention on chewing and swallowing behaviors in healthy humans. *Scientific Reports* **9** (2019) 1–9
- [46] Ding, R., Larson, C.R., Logemann, J.A., Rademaker, A.W.: Surface electromyographic and electroglottographic studies in normal subjects under two swallow conditions: Normal and during the Mendelsohn maneuver. *Dysphagia* **17** (2002) 1–12

- [47] Reyes, A., Cruickshank, T., Thompson, J., Ziman, M., Nosaka, K.: Surface electromyograph activity of submental muscles during swallowing and expiratory muscle training tasks in Huntington's disease patients. *Journal of Electromyography and Kinesiology* **24** (2014) 153–158
- [48] Fassicollo, C.E., Machado, B.C.Z., Garcia, D.M., de Felício, C.M.: Swallowing changes related to chronic temporomandibular disorders. *Clinical Oral Investigations* **23** (2019) 3287–3296
- [49] Poorjavad, M., Moghadam, S.T., Ansari, N.N.: Effects of the head lift exercise and neuromuscular electrical stimulation on swallowing muscles activity in healthy older adults: A randomized pilot study. *Clinical Interventions in Aging* **14** (2019) 1131–1140
- [50] Hermens, H.J., Merletti, R., Rix, H., Freriks, B.: The state of the art on signal processing methods for surface electromyography. Roessingh Research and Development, Enschede (1999)
- [51] Roy, S.H., Bonato, P., Knafitz, M.: Emg assessment of back muscle function during cyclical lifting. *Journal of Electromyography and Kinesiology* **8** (1998) 233–245
- [52] Restrepo-Agudelo, S., Roldan-Vasco, S., Ramirez-Arbelaez, L., Cadavid-Arboleda, S., Perez-Giraldo, E., Orozco-Duque, A.: Improving surface EMG burst detection in infrahyoid muscles during swallowing using digital filters and discrete wavelet analysis. *Journal of Electromyography and Kinesiology* **35** (2017) 1–8
- [53] Yüksel, A., Kulan, C.A., Akçiçek, F.: The investigation of asymptomatic swallowing disorder through surface electromyography in the geriatric population. *Aging Clinical and Experimental Research* (2019)
- [54] Mao, S., Zhang, Z., Khalifa, Y., Donohue, C., Coyle, J.L., Sejdic, E.: Neck sensor-supported hyoid bone movement tracking during swallowing. *Royal Society Open Science* **6** (2019)
- [55] Sejdíć, E., Movahedi, F., Zhang, Z., Kurosu, A., Coyle, J.L.: The effects of compressive sensing on extracted features from tri-axial swallowing accelerometry signals. *Compressive Sensing V: From Diverse Modalities to Big Data Analytics* **9857** (2016) 985704
- [56] Rebrion, C., Zhang, Z., Khalifa, Y., Ramadan, M., Kurosu, A., Coyle, J.L., Perera, S., Sejdic, E.: High-Resolution Cervical Auscultation Signal Features Reflect Vertical and Horizontal Displacements of the Hyoid Bone during Swallowing. *IEEE Journal of Translational Engineering in Health and Medicine* **7** (2019)

-
- [57] Dudik, J.M., Kurosu, A., Coyle, J.L., Sejdić, E.: Dysphagia and its effects on swallowing sounds and vibrations in adults. *BioMedical Engineering Online* **17** (2018) 1–18
- [58] Steele, C.M., Sejdić, E., Chau, T.: Noninvasive detection of thin-liquid aspiration using dual-axis swallowing accelerometry. *Dysphagia* **28** (2013) 105–112
- [59] Dudik, J.M., Jestrović, I., Luan, B., Coyle, J.L., Sejdić, E.: A comparative analysis of swallowing accelerometry and sounds during saliva swallows. *BioMedical Engineering Online* **14** (2015) 1–15
- [60] Lee, J., Steele, C.M., Chau, T.: Time and time-frequency characterization of dual-axis swallowing accelerometry signals. *Physiological Measurement* **29** (2008) 1105–1120
- [61] Sejdić, E., Steele, C.M., Chau, T.: Segmentation of dual-axis swallowing accelerometry signals in healthy subjects with analysis of anthropometric effects on duration of swallowing activities. *IEEE Transactions on Biomedical Engineering* **56** (2009) 1090–1097
- [62] Dudik, J.M., Coyle, J.L., El-Jaroudi, A., Mao, Z.H., Sun, M., Sejdić, E.: Deep learning for classification of normal swallows in adults. *Neurocomputing* **285** (2018) 1–9
- [63] Jestrović, I., Coyle, J.L., Sejdić, E.: The effects of increased fluid viscosity on stationary characteristics of EEG signal in healthy adults. *Brain Research* **1589** (2014) 45–53
- [64] Sejdić, E., Steele, C.M., Chau, T.: A method for removal of low frequency components associated with head movements from dual-axis swallowing accelerometry signals. *PLoS ONE* **7** (2012) 1–8
- [65] Wang, Z., Willett, P.: Two algorithms to segment white Gaussian data with piecewise constant variances. *IEEE Transactions on Signal Processing* **51** (2003) 373–385
- [66] Mamun, K.A., Steele, C.M., Chau, T.: Swallowing accelerometry signal feature variations with sensor displacement. *Medical Engineering and Physics* **37** (2015) 665–673
- [67] Lee, J., Steele, C.M., Chau, T.: Swallow segmentation with artificial neural networks and multi-sensor fusion. *Medical Engineering and Physics* **31** (2009) 1049–1055
- [68] Zoratto, D.C.B., Chau, T., Steele, C.M.: Hyolaryngeal excursion as the physiological source of swallowing accelerometry signals. *Physiological Measurement* **31** (2010) 843–855
- [69] Sejdić, E., Komisar, V., Steele, C.M., Chau, T.: Baseline characteristics of dual-axis cervical accelerometry signals. *Annals of Biomedical Engineering* **38** (2010) 1048–1059
- [70] Sejdić, E., Orovi, I., Stankovi, S., Chau, T., Steele, C.M.: Time-frequency analysis and hermite projection method applied to swallowing accelerometry signals. *Eurasip Journal on Advances in Signal Processing* **2010** (2010)

- [71] Zohouri Haghian, N.: Characterization and Segmentation of Acoustic Swallowing Signals Collected Concurrently with Dual-axis Accelerometry. PhD thesis, University of Toronto (2014)
- [72] Mohammadi, H., Samadani, A.A., Steele, C., Chau, T.: Automatic discrimination between cough and non-cough accelerometry signal artefacts. *Biomedical Signal Processing and Control* **52** (2019) 394–402
- [73] Sejdić, E., Falk, T.H., Steele, C.M., Chau, T.: Vocalization removal for improved automatic segmentation of dual-axis swallowing accelerometry signals. *Medical Engineering and Physics* **32** (2010) 668–672
- [74] Steele, C.M., Mukherjee, R., Kortelainen, J.M., Pölönen, H., Jedwab, M., Brady, S.L., Theimer, K.B., Langmore, S., Riquelme, L.F., Swigert, N.B., Bath, P.M., Goldstein, L.B., Hughes, R.L., Leifer, D., Lees, K.R., Meretoja, A., Muehleman, N.: Development of a Non-invasive Device for Swallow Screening in Patients at Risk of Oropharyngeal Dysphagia: Results from a Prospective Exploratory Study. *Dysphagia* **34** (2019) 698–707
- [75] Schultheiss, C., Schauer, T., Nahrstaedt, H., Seidl, R.O.: Automated detection and evaluation of swallowing using a combined emg/bioimpedance measurement system. *Scientific World Journal* **2014** (2014)
- [76] Khmag, A., Al-Haddad, S.A.R., Hashim, S.J.B., et al.: Additive and multiplicative noise removal based on adaptive wavelet transformation using cycle spinning. *American Journal of Applied Sciences* **11** (2014) 316
- [77] Mert, A., Kılıç, N., Akan, A.: Evaluation of bagging ensemble method with time-domain feature extraction for diagnosing of arrhythmia beats. *Neural Computing and Applications* **24** (2014) 317–326
- [78] Phinyomark, A., Phukpattaranont, P., Limsakul, C.: Feature reduction and selection for emg signal classification. *Expert systems with applications* **39** (2012) 7420–7431
- [79] Huang, H.P., Chen, C.Y.: Development of a myoelectric discrimination system for a multi-degree prosthetic hand. In: *Proceedings 1999 IEEE International Conference on Robotics and Automation (Cat. No. 99CH36288C)*. Volume 3., IEEE (1999) 2392–2397
- [80] Hudgins, B., Parker, P., Scott, R.N.: A new strategy for multifunction myoelectric control. *IEEE transactions on biomedical engineering* **40** (1993) 82–94
- [81] Kim, K.S., Choi, H.H., Moon, C.S., Mun, C.W.: Comparison of k-nearest neighbor, quadratic discriminant and linear discriminant analysis in classification of electromyogram signals based on the wrist-motion directions. *Current applied physics* **11** (2011) 740–745

- [82] Philipson, L.: The electromyographic signal used for control of upper extremity prostheses and for quantification of motor blockade during epidural anaesthesia. PhD thesis, VTT Grafiska (1987)
- [83] Solnik, S., Rider, P., Steinweg, K., DeVita, P., Hortobágyi, T.: Teager–kaiser energy operator signal conditioning improves emg onset detection. *European journal of applied physiology* **110** (2010) 489–498
- [84] Lee, J., Steele, C., Chau, T.: Time and time–frequency characterization of dual-axis swallowing accelerometry signals. *Physiological measurement* **29** (2008) 1105
- [85] Kashyap, K.H., Shenoy, U.J.: Classification of power system faults using wavelet transforms and probabilistic neural networks. In: *Proceedings of the 2003 International Symposium on Circuits and Systems, 2003. ISCAS'03. Volume 3.*, IEEE (2003) III–III
- [86] Rosso, O.A., Blanco, S., Yordanova, J., Kolev, V., Figliola, A., Schürmann, M., Başar, E.: Wavelet entropy: a new tool for analysis of short duration brain electrical signals. *Journal of neuroscience methods* **105** (2001) 65–75
- [87] Rosenstein, M.T., Collins, J.J., De Luca, C.J.: A practical method for calculating largest lyapunov exponents from small data sets. *Physica D: Nonlinear Phenomena* **65** (1993) 117–134
- [88] Richman, J.S., Moorman, J.R.: Physiological time-series analysis using approximate entropy and sample entropy. *American Journal of Physiology-Heart and Circulatory Physiology* **278** (2000) H2039–H2049
- [89] Lempel, A., Ziv, J.: On the complexity of finite sequences. *IEEE Transactions on information theory* **22** (1976) 75–81
- [90] Visa, S., Ramsay, B., Ralescu, A.L., Van Der Knaap, E.: Confusion matrix-based feature selection. *MAICS* **710** (2011) 120–127
- [91] Buntine, W.L., Jakulin, A.: Applying discrete pca in data analysis. *arXiv preprint arXiv:1207.4125* (2012)
- [92] Buntine, W.: Variational extensions to em and multinomial pca. In: *European Conference on Machine Learning*, Springer (2002) 23–34
- [93] Cai, Y., Huang, T., Hu, L., Shi, X., Xie, L., Li, Y.: Prediction of lysine ubiquitination with mRMR feature selection and analysis. *Amino Acids* **42** (2012) 1387–1395
- [94] Sulaiman, M.A., Labadin, J.: Feature selection based on mutual information. In: *2015 9th International Conference on IT in Asia (CITA)*, IEEE (2015) 1–6

- [95] Maxwell, A.E., Warner, T.A., Fang, F.: Implementation of machine-learning classification in remote sensing: An applied review. *International Journal of Remote Sensing* **39** (2018) 2784–2817
- [96] Taud, H., Mas, J.: Multilayer perceptron (mlp). In: *Geomatic Approaches for Modeling Land Change Scenarios*. Springer (2018) 451–455
- [97] Cheng, F., Yang, C., Zhou, C., Lan, L., Zhu, H., Li, Y.: Simultaneous determination of metal ions in zinc sulfate solution using uv–vis spectrometry and spse-xgboost method. *Sensors* **20** (2020) 4936
- [98] LaValle, S.M., Branicky, M.S., Lindemann, S.R.: On the relationship between classical grid search and probabilistic roadmaps. *The International Journal of Robotics Research* **23** (2004) 673–692
- [99] Sebastian, R.V., Estefania, P.G., Andres, O.D.: Scalogram-energy based segmentation of surface electromyography signals from swallowing related muscles. *Computer methods and programs in biomedicine* **194** (2020) 105480
- [100] Yoon, K.J., Park, J.H., Park, J.H., Jung, I.S.: Videofluoroscopic and manometric evaluation of pharyngeal and upper esophageal sphincter function during swallowing. *Journal of neurogastroenterology and motility* **20** (2014) 352
- [101] Kreisler, L., Fain, M., Soulé, M.: La clinique psychosomatique de l’enfant. a propos des troubles fonctionnels du nourrisson: coliques idiopathiques du premier trimestre, insomnie, mérycisme, anorexie, vomissements. *La Psychiatrie de l’enfant* **9** (1966) 89
- [102] Boiron, M., Rouleau, P., Metman, E.: Exploration of pharyngeal swallowing by audio-signal recording. *Dysphagia* **12** (1997) 86–92
- [103] Klahn, M.S., Perlman, A.L.: Temporal and durational patterns associating respiration and swallowing. *Dysphagia* **14** (1999) 131–138
- [104] Martin, B., Logemann, J., Shaker, R., Dodds, W.: Coordination between respiration and swallowing: respiratory phase relationships and temporal integration. *Journal of applied physiology* **76** (1994) 714–723
- [105] Maria das Graças, W., Belo, L.R., Carneiro, D., Asano, A.G., Oliveira, P.J.A., da Silva, D.M., Lins, O.G.: Swallowing in patients with parkinson disease: a surface electromyography study. *Dysphagia* **27** (2012) 550–555
- [106] Hackett, J.K., Shah, M.: Multi-sensor fusion: a perspective. In: *Proceedings., IEEE International Conference on Robotics and Automation, IEEE* (1990) 1324–1330

- [107] Mohammadi, H., Samadani, A.A., Steele, C., Chau, T.: Automatic discrimination between cough and non-cough accelerometry signal artefacts. *Biomedical Signal Processing and Control* **52** (2019) 394–402
- [108] Kurosu, A., Coyle, J.L., Dudik, J.M., Sejdic, E.: Detection of swallow kinematic events from acoustic high-resolution cervical auscultation signals in patients with stroke. *Archives of physical medicine and rehabilitation* **100** (2019) 501–508